い。

ドパミンは，黒質線条体系以外に，中脳腹側被蓋野から大脳辺縁系に至る報酬系にも関連する神経伝達物質である。この系は報酬，すなわち“行動の動機づけ”に関係し，人間の感情の“快感”や“嬉しさ”とかかわっていることもわかってきた。よく笑い，楽しく喜ぶことで，このもう一つのドパミン系が強く賦活される。報酬系にかかわるドパミンの活性化が，PD 予防に関連するというデータはないが，人生を大いにエンジョイし，大脳のドパミン系の活性化を心がけたいものである。

●文　献

1）Mizuta I, Satake W, Nakabayashi Y, et al : Multiple candidate gene analysis identifies alpha-synuclein as a susceptibility gene for sporadic Parkinson's disease. Hum Mol Genet **15** : 1151-1158, 2006

2）Hernan MA, Takkouche B, Caamano-Isorna F, et al : A meta-analysis of coffee drinking, cigarette smoking, and the risk of Parkinson's disease. Ann Neurol **52** : 276-284, 2002

3）Allam MF, Campbell MJ, Hofman A, et al : Smoking and Parkinson's disease : systematic review of prospective studies. Mov Disord **19** : 614-621, 2004

4）Hancock DB, Martin ER, Stajich JM, et al : Smoking, caffeine, and nonsteroidal anti-inflammatory drugs in families with Parkinson disease. Arch Neurol **64** : 576-580, 2007

5）Hernan MA, Chen H, Schwarzschild MA, et al : Alcohol consumption and the incidence of Parkinson's disease. Ann Neurol **54** : 170-175, 2003

6）Jimenez-Jimenez FJ, Mateo D, Gimenez-Roldan S : Premorbid smoking, alcohol consumption, and coffee drinking habits in Parkinson's disease : a case-control study. Mov Disord **7** : 339-344, 1992

7）Menza M : The personality associated with Parkinson's disease. Curr Psychiatry Rep **2** : 421-426, 2000

Am J Physiol Gastrointest Liver Physiol 296: G23–G35, 2009.
First published November 20, 2008; doi:10.1152/ajpgi.90225.2008.

Requirement of Notch activation during regeneration of the intestinal epithelia

Ryuichi Okamoto,[1,2] Kiichiro Tsuchiya,[2] Yasuhiro Nemoto,[2] Junko Akiyama,[2] Tetsuya Nakamura,[1,2] Takanori Kanai,[2] and Mamoru Watanabe[2]

[1]*Department of Advanced Therapeutics in Gastrointestinal Diseases and* [2]*Department of Gastroenterology and Hepatology, Graduate School, Tokyo Medical and Dental University, Tokyo, Japan*

Submitted 7 March 2008; accepted in final form 18 November 2008

Okamoto R, Tsuchiya K, Nemoto Y, Akiyama J, Nakamura T, Kanai T, Watanabe M. Requirement of Notch activation during regeneration of the intestinal epithelia. *Am J Physiol Gastrointest Liver Physiol* 296: G23–G35, 2009. First published November 20, 2008; doi:10.1152/ajpgi.90225.2008.—Notch signaling regulates cell differentiation and proliferation, contributing to the maintenance of diverse tissues including the intestinal epithelia. However, its role in tissue regeneration is less understood. Here, we show that Notch signaling is activated in a greater number of intestinal epithelial cells in the inflamed mucosa of colitis. Inhibition of Notch activation in vivo using a γ-secretase inhibitor resulted in a severe exacerbation of the colitis attributable to the loss of the regenerative response within the epithelial layer. Activation of Notch supported epithelial regeneration by suppressing goblet cell differentiation, but it also promoted cell proliferation, as shown in in vivo and in vitro studies. By utilizing tetracycline-dependent gene expression and microarray analysis, we identified a novel group of genes that are regulated downstream of Notch1 within intestinal epithelial cells, including PLA2G2A, an antimicrobial peptide secreted by Paneth cells. Finally, we show that these functions of activated Notch1 are present in the mucosa of ulcerative colitis, mediating cell proliferation, goblet cell depletion, and ectopic expression of PLA2G2A, thereby contributing to the regeneration of the damaged epithelia. This study showed the critical involvement of Notch signaling during intestinal tissue regeneration, regulating differentiation, proliferation, and antimicrobial response of the epithelial cells. Thus Notch signaling is a key intracellular molecular pathway for the proper reconstruction of the intestinal epithelia.

intestinal epithelial cells; goblet cells; PLA2G2A; ulcerative colitis

THE INTESTINAL EPITHELIA are composed of four lineages of intestinal epithelial cells (IECs) that arise from intestinal stem cells (1). Recent studies have shown that various signals such as Wnt, Sonic hedgehog, and bone morphogenetic protein interact within the stem and progenitor cells of the intestinal epithelia to finely regulate the expansion and the cell fate decision of IECs. Other studies have revealed that Notch signaling may also play critical roles in the maintenance of the intestinal epithelia (20).

Notch signaling is a signaling pathway known to regulate differentiation and proliferation of cells in diverse adult tissues (1). Activation of Notch receptor is mediated by the cleavage of its intracellular domain (NICD), and this intracellular domain translocates from the cell membrane to the nucleus, thereby functioning as a transcriptional activator of target genes such as Hes1 (10, 25). The functional role of Notch signaling in the intestine was first described in a study of Hes1-null mice; depletion of Hes1 was associated with significant increases in the secretory lineage IECs (9). Other studies have shown that the activation of Notch promoted proliferation of crypt progenitor cells and directed their cell fates toward absorptive but not secretory lineage cells (6, 28, 33). A recent study suggested that Notch might also function in postmitotic IECs, directing their cell fates toward secretory lineage cells (42). Thus these studies have suggested that Notch signaling functions in the intestine to regulate differentiation and proliferation of IECs, contributing to the maintenance and the homeostasis of the intestinal mucosa. However, the role of Notch signaling in tissue regeneration is less understood.

Damage of the intestinal epithelia is observed in a wide variety of diseases, such as acute intestinal infections, radiation injuries, or idiopathic inflammatory bowel diseases (23). Once the epithelial layer is damaged, it responds by restoring the continuity and integrated structure via activating the stepwise regeneration program (16). The initial response is called restitution, which is the redistribution of remaining IECs to rapidly cover the damaged area. This initial step is usually completed in an extremely short period of time and thus does not require the proliferation or expansion of IECs (19). However, in the next step, the rapid expansion of IECs is necessary to rebuild the proper structure of the epithelia. This response is manifested by the appearance of the regenerative epithelia in the intestine, showing a marked expansion of the proliferating compartment consisting of undifferentiated IECs. However, the exact molecular mechanisms involved in this critical step of intestinal epithelial regeneration has never been described.

Another change that is observed in the intestine during such a regenerative process is the ectopic expression of antimicrobial peptides by IECs. Paneth cells usually secrete peptides such as lysozymes, α-defensins, or PLA2G2A, and this helps to maintain the ideal environment for the stem and progenitor IECs within the small intestinal crypts. The ectopic expressions of these antimicrobial peptides by IECs are frequently observed in the inflamed colonic mucosa (5, 8), and such expressions likely support the local immune system in providing an ideal environment for the regeneration of the damaged mucosa.

In this study, we show that Notch signaling is activated in many IECs in the inflamed mucosa of murine colitis. Results show that the activation of Notch is critical for the proper regeneration program in the epithelial layer and that it helps to suppress goblet cell differentiation and promote cell proliferation. A comprehensive analysis identified a novel group of genes regulated by Notch in IECs, which included

Address for reprint requests and other correspondence: M. Watanabe, Dept. of Gastroenterology and Hepatology, Graduate School, Tokyo Medical and Dental Univ., 1-5-45 Yushima, Bunkyo-ku, Tokyo 113-8519, Japan (e-mail address: mamoru.gast@tmd.ac.jp).

The costs of publication of this article were defrayed in part by the payment of page charges. The article must therefore be hereby marked "*advertisement*" in accordance with 18 U.S.C. Section 1734 solely to indicate this fact.

a gene encoding an antimicrobial peptide called PLA2G2A. Such functions of Notch activation were present not only in the mice intestine but also in the human intestine. Finally, the clinical relevance of Notch-mediated regeneration is analyzed in ulcerative colitis (UC). Thus Notch signaling is a key-signaling pathway involved in intestinal tissue regeneration, in fine regulation of differentiation and proliferation, and in antimicrobial activities in IECs. Our findings point to a novel molecular target for agents that could promptly regenerate the intestinal mucosa in a wide range of intestinal diseases.

MATERIALS AND METHODS

Mice. C57BL/6J mice at 8 wk of age were purchased from Japan Clea. Mice were housed and maintained in the animal facility of Tokyo Medical and Dental University. The institutional animal use and care committee approved the study.

In vivo experiments. Induction of colitis was performed as previously described (17). Briefly, mice were fed ad libitum with 1.75% dextran sodium sulfate (DSS, Bio Research of Yokohama) for 5 consecutive days, followed by distilled water for another 5 days. For inhibition of Notch activation, mice were orally administered with either 5% DMSO (vehicle, VEC) or LY411,575 (LY) (10 mg/kg) dissolved in 0.5% (wt/vol) methylcellulose (WAKO), once daily for 5 consecutive days. Twenty-four mice were separated into four groups: *1*) fed distilled water for five days followed by daily administration of vehicle alone (VEC, $n = 6$) for 5 days, *2*) fed distilled water for 5 days followed by daily administration of LY411,575 (LY, $n = 6$) for five days, *3*) fed 1.75% DSS for 5 days followed by daily administration of vehicle (DSS + VEC, $n = 6$) for 5 days, and *4*) fed 1.75% DSS for 5 days followed by daily administration of LY411,575 (DSS + LY, $n = 6$) for 5 days. The whole body weights of mice were measured everyday. They were euthanized 12 h after the final administration. Colonic tissues were subjected to hematoxylin and eosin staining and analyzed by histological scoring following the criteria described elsewhere (21). Flow cytometry of thymocytes and splenocytes were performed as previously described (35, 41).

Immunoblot analysis. Immunoblots were performed as described elsewhere (18). The primary antibodies used were anti-Cleaved Notch1 (1:1,000, Cell Signaling Technology), anti-Hes1 (1:4,000, a kind gift from Dr. T. Sudo), and anti-β-actin (1:5,000, Sigma). Proteins were visualized either by the ECL Advance Western Blotting Kit (GE Healthcare) or ECL Western Blotting Kit (GE Healthcare).

Cell culture. The cell cultures and transfections of plasmid DNA were performed as described elsewhere (18). The inhibition of Notch signaling was achieved by the addition of LY411,575 (1 μM), synthesized according to Wu et al. (38). A cell line expressing Notch1 intracellular domain (Tet-On NICD1 cells) under the control of tetracycline or doxycycline (DOX, 100 ng/ml, Clontech) was generated as described elsewhere (18), using LS174T cells as parent cells. The cell lines were supplemented with Blastcidin (7.5 μg/ml, Invitrogen) and Zeocin (750 μg/ml, Invitrogen) for their maintenance.

RT-PCR assays. RT-PCR was performed as described elsewhere (18). Quantitative analyses using the SYBR green master mix (Qiagen) was performed by ABI 7500 (Applied Biosystems). Primer sequences for human β-actin, G3PDH, or MUC2 have been previously described (30). The primer sequences for other genes are summarized in Table 1. The results are shown as the means of the data collected from two rounds of assays, with each assay performed in triplicate. The data were statistically analyzed with paired Student's *t*-tests.

Human intestinal tissue specimens. Human tissue specimens were obtained from patients who underwent surgery for the treatment of Crohn's disease, UC, or colon cancer at Yokohama Municipal General Hospital or Tokyo Medical and Dental University Hospital. Written informed consent was obtained from each patient, and the study was approved by the ethics committee of Yokohama Municipal General Hospital and Tokyo Medical and Dental University.

Immunohistochemistry. Immunohistochemistry using intestinal tissues has been described elsewhere (12). The same antibodies used in immunoblot analysis were also used for the immunohistological staining of NICD1 and Hes1. The other antibodies used were anti-human Ki-67 (1:50, MIB-1, DAKO), anti-human PLA2G2A (1:200, sc-14468, Santa Cruz Biotechnology), anti-human MUC2 (1:100, Ccp58, Santa Cruz Biotechnology), and anti-mouse Ki-67 (1:50, TEC-3, DAKO). Microwave treatment (500 W, 10 min) in 10 mM citrate buffer was required for staining human tissues in Hes1, Ki-67, and NICD1 and for staining mice tissues in Ki-67. The tyramide signal amplification (Molecular Probes) was used for immunofluorescent detection of NICD1. Staining was visualized by an avidin-biotin-peroxidase complex (ABC) elite kit (Vector) using diaminobenzidine as a substrate or by secondary antibodies conjugated with Alexa-594 or Alexa-488 (Molecular Probes). The quantification of Hes1 (Fig. 1*B*), Alcian blue, Ki-67, or NICD1 (Fig. 8*B*) was conducted by the examination of nine randomly selected longitudinal sections of crypts selected from at least three different individuals. The data were statistically analyzed with paired Student's *t*-tests.

Microarray. Microarray analysis was performed using the Acegene human oligo chip 30K subset A (Hitachi software). Total RNA was collected before and after 24 h of NICD1 expression in LS174T cells and labeled using the Amino Aryll Message Amp aRNA kit (Ambion). The complete dataset of the analysis has been submitted to the NCBI Gene Expression Omnibus (GEO) and is accessible through GEO accession number GSE10136.

Table 1. *Primers used in the present study*

Gene	Primer Sequence	
	Forward	Reverse
Human Hes1	5'- ATGCCAGCTGATATAATGGAG -3'	5'- TCACGTCGTTCATGCACTCG -3'
Human Notch1	5'- CCGAACCAATACAACCGTCT -3'	5'- GCGATCTCGGACTGCTGCATGCT -3'
Human PLA2G2A	5'- ACCATGAAGACCCTCCTACTG -3'	5'- GAAGAGGGAGTCAGCAACG -3'
Mouse Hes1	5'- TCAACACGACACCGGACAAACC -3'	5'- GGTACTTCCCCAACACGCTCG -3'
Mouse MUC2	5'- TCCACCATGGGGCTGCCAGT -3'	5'- GGCCCGAGAGTAGACCTTGG -3'
Mouse TNF-α	5'- CTACTGCGCGTGCCAAGGCTGT -3'	5'- GCCATGAGGTCCACCACGCTG -3'
Mouse IFN-γ	5'- ACACTGCATCTTGGCTTTGC -3'	5'- CGGATGAGCTCATTGAATGCT -3'
MouseIL-1α	5'- CCCGTCGTTAAAGCTGTCTG -3'	5'- AATTGGAATCCAGGGGAAAC -3'
Mouse IL-1β	5'- TTGACGGACCCCAAAAGAT -3'	5'- GAAGCTGGATGCTCTCATCTG -3'
Mouse IL-6	5'- GCTACCAAACTGGATATAATCAGGA -3'	5'- CCAGGTAGCTATGGTACTCCAGAA -3'
Mouse PLA2G2A	5'- AAGAAGCCCAAATGCTGAAA -3'	5'- TTTATCACCGGGAAACTTGG -3'
Mouse β-actin	5'- CCTAAGGCCAACCGTGAAAAG -3'	5'- TGTTCATGGTGCTAGGAGCCA -3'

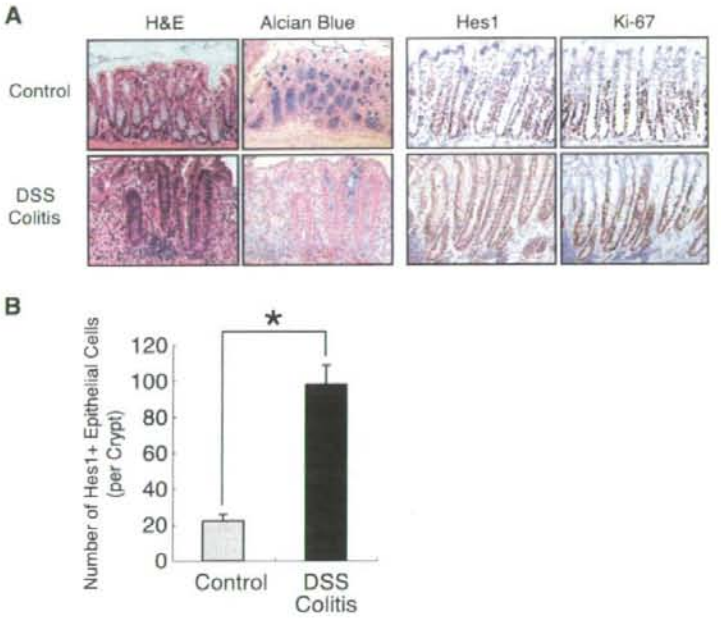

Fig. 1. Activation of Notch signaling is increased in crypts of dextran sodium sulfate (DSS)-induced colitis. *A*: histological analysis of DSS-induced colitis showing a decrease in mucin-producing intestinal epithelial cells (IECs) and an increase in Hes1- and Ki-67-expressing IECs within the crypts of the colitic mucosa. Blue staining with Alcian blue represents mucin production, whereas brown staining with diaminobenzidine (DAB) shows positive staining for Hes1 or Ki-67 (original magnification ×400). *B*: quantitative analysis of Hes1-positive IECs in crypts of normal or colitic mucosa. Data are shown as number of Hes1-positive cells per crypt on the basis of the analysis of immunohistochemical stainings. Error bars represent SD. $*P < 0.05$ on the Student's *t*-test. H & E, hematoxylin and eosin.

Plasmids. Hes1p-Luc, containing six tandem-repeats of the RBP-Jk binding site, was a kind gift from Dr. Kageyama (Kyoto, Japan). PLA2-Luc was generated by cloning a 2778-bp sequence 5′ of the human PLA2G2A gene (corresponding to −2,758 to + 20 of the promoter region) into a pGL3 basic vector (Promega). MUC2-Luc (40) was a kind gift from Dr. Yuasa (Tokyo, Japan). Tetracycline-dependent expression of NICD1 was achieved by cloning the gene encoding the intracellular portion of the mouse Notch1 (amino acid 1,704-2,531) into the pcDNA4/TO/myc-his vector (Invitrogen). All constructs were confirmed by DNA sequencing.

Immunostaining of cultured cells. Staining of cultured cells has been previously described (30). Detection of the MUC2 antibody was carried out either by the standard ABC method or by the Alexa 594-conjugated secondary antibody (Molecular Probes). The quantification of cells positive for MUC2 staining was performed by examining six randomly selected fields (three fields each in two individual counts) under ×400 magnification. The data were statistically analyzed with paired Student's *t*-tests.

ELISA. For PLA2G2A protein quantification, 1×10^6 cells were cultured in 2 ml of medium with or without DOX and analyzed with the human-PLA2 enzyme immunoassay kit (Cayman Chemicals). The incorporation of BrdU was examined by seeding cells at various cell densities in the 96-well plate, supplemented with DMSO or LY411,575. The BrdU was added 8 h before the end of culture, and the cells were subjected to analysis with the cell proliferation ELISA kit (Roche Diagnostics). The results are shown as the means of data collected by two rounds of assays, with each assay performed in triplicate. The data were statistically analyzed with paired Student's *t*-tests.

Reporter assays. The reporter assay was performed as previously described (18). Each assay was performed in triplicate, and the results were normalized using the *Renilla* luciferase activity. The results are shown as the means of normalized arbitrary units, and the data were statistically analyzed with paired Student's *t*-tests.

RESULTS

Hes1 is expressed in crypt epithelial cells of DSS-colitis. Since previous studies have evaluated the contribution of Notch signaling in the maintenance of mice intestinal epithelium (28, 33, 34), we sought to examine the role of Notch signaling in mice colitis. At first, we analyzed the expression of Hes1, a direct target gene of Notch, in mice with colitis induced by the oral administration of DSS (DSS-colitis, Fig. 1*A*). In the normal colon, crypts are predominantly composed of mature goblet cells that produce mucin. In such crypts, Hes1 is expressed in IECs residing at the lowest part of the crypt, which is also where Ki-67-positive IECs are found. In sharp contrast, the clear loss of mucin production was observed in the inflamed mucosa of DSS-colitis mice. The expressions of both Hes1 and Ki-67 were observed in a larger population of IECs, which were distributed from the bottom to the most upper regions of the crypt, suggesting that Notch signaling was activated in these IECs. The quantitative analysis of the immunostaining revealed significant increases in Hes1-positive IECs within the crypts of the DSS-colitis mice (Fig. 1*B*). These findings suggested that Notch signaling is activated in a greater number of IECs in DSS-colitis, which might be closely related with the greater number of proliferating IECs and the loss of mucin-producing IECs.

LY411,575 inhibits Notch activation and promotes goblet cell differentiation in mice intestine. To further examine the role of Notch signaling in colitis, we used LY411,575, a γ-secretase inhibitor (GSI) that is known to block Notch activation in vivo (14, 27, 36). Oral administration of LY411,575 for 5 consecutive days significantly reduced the expression of

Hes1 mRNA in mice intestine, suggesting that Notch activation was inhibited (Fig. 2*A*). In contrast, the expression of MUC2 mRNA was significantly increased by LY411,575, suggesting that the number of goblet cells increased. Consistent with this, histological analysis showed marked increases in mucus-producing IECs in the intestines of the LY411,575-treated mice (Fig. 2*C*). Consistent with reports from previous studies (27, 36), these results showed that LY411,575 could

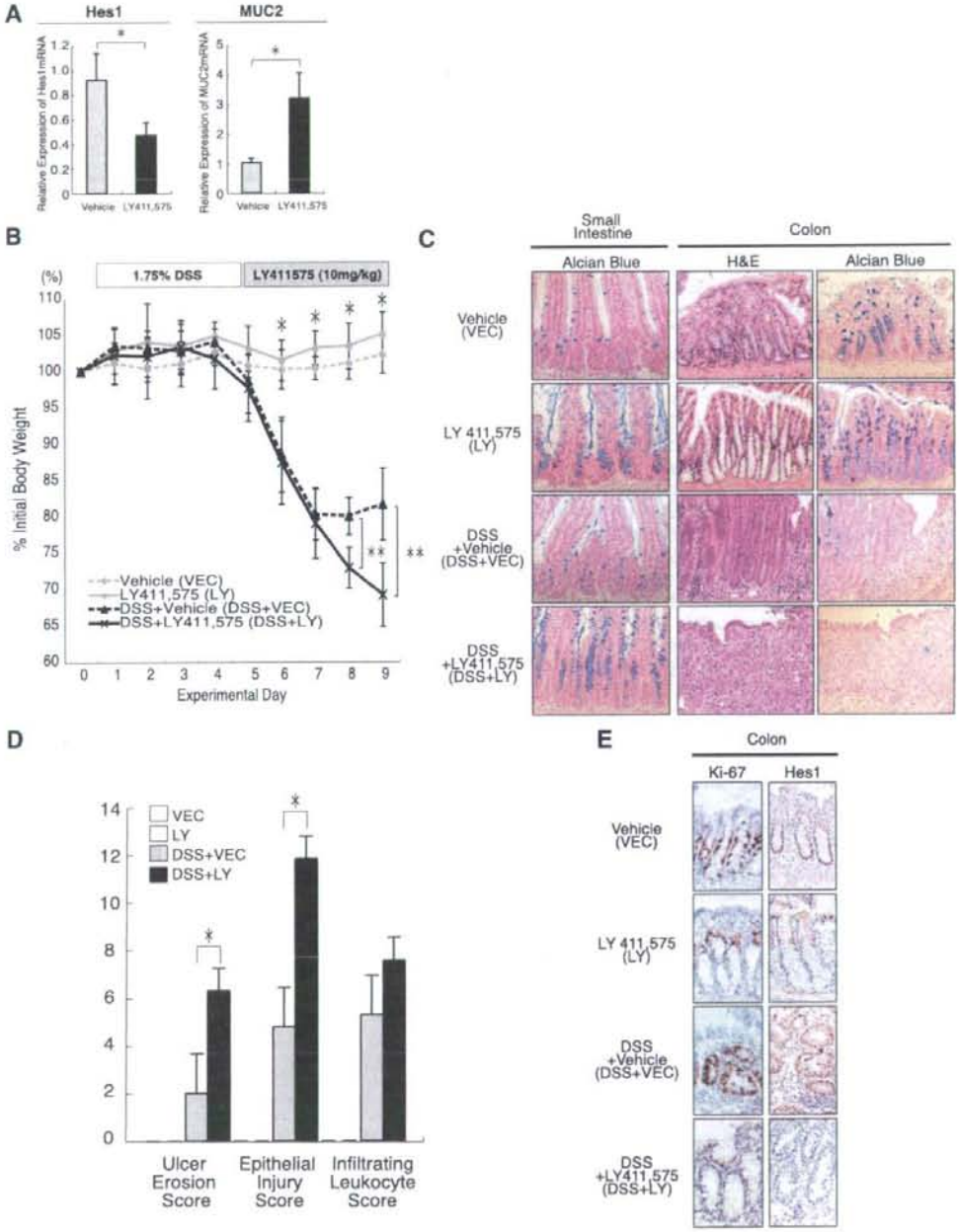

simultaneously inhibit Notch activation and promote differentiation to goblet cells in the mice intestine.

We also found marked atrophy of the thymus in LY411,575-treated mice (Supplemental Fig. S1*A*). Supplemental data for this article are available on the *American Journal of Physiology Gastrointestinal and Liver Physiology* website. Further analysis of the thymus revealed that the total number of thymocytes was significantly reduced (Supplemental Fig. S1*B*) and that the tissue architecture was disrupted (Supplemental Fig. S1*C*). Analysis of CD4/CD8 expression revealed a significant proportional reduction in double-positive cells (Supplemental Fig. S1*D*) and a reduction in the absolute number of cells (Supplemental Fig. S1*E*), suggesting that there was a significant loss of immature cells in the thymus with LY411,575 treatment. However, such an effect of LY411,575 was not present in the spleen (Supplemental Fig. S1, *A–E*). These findings clearly showed that the LY411,575 treatment had a systemic effect, affecting the thymus in addition to the intestine.

LY411,575 exacerbates DSS-colitis by impairing epithelial regeneration. Using the methods described, we designed an experiment to examine the effect of Notch inhibition during colitis (Fig. 2*B*). Mice were separated into four groups: vehicle alone (VEC), LY411,575 alone (LY), DSS with vehicle (DSS + VEC), and DSS with LY411,575 (DSS + LY). As of *day 5*, the total body weights showed significant reductions from *day 0* in DSS-treated mice (Fig. 2*B*) compared with the weights of those without DSS (the day when DSS treatment was started is designated as *day 0*). However, the DSS + LY mice showed even greater reductions in weight as of *day 8*; their reductions in body weight were significantly greater than the weight reductions in DSS + VEC mice (Fig. 2*B*). This severe loss of body weight observed in DSS + LY mice was also fatal because two mice in this group were dead at the time of euthanasia (fatality rate = 2/6, 33.3%). No deaths were observed in any other experimental group. These results suggested that LY411,575 significantly exacerbates the clinical course of DSS-colitis. A histological analysis of LY or DSS + LY mice showed a marked increase in goblet cells in the small intestine, confirming the effect of LY411,575 treatment (Fig. 2*C*). The increase in goblet cells was also observed in the colon of LY mice. A histological analysis of DSS + VEC mice showed a clear induction of colitis, as shown by the marked increase in inflammatory cells and the elongation of goblet cell depleted crypts. However, in sharp contrast, DSS + LY mice showed a severe loss of the epithelial layer in addition to an infiltration of inflammatory cells, which appeared to lack signs of epithelial regeneration (Fig. 2*C*). A histological scoring of the colonic tissues revealed increased ulcer formation and epithelial injury in DSS + LY mice compared with DSS + VEC mice, whereas no significant changes were observed in the degree of inflammation (Fig. 2*D*). Consistent with this, the mRNA expression of proinflammatory cytokines was increased in the colon of DSS-treated mice, but no clear differences were observed between DSS + VEC and DSS + LY mice (Supplemental Fig. S2).

For further analysis, we examined the expression of Hes1 and Ki-67 in the inflamed region of the colonic tissues. An increase in Hes1- or Ki-67-positive IECs was confirmed in DSS + VEC mice (Fig. 2*E*). However, both Hes1 and Ki-67 expression appeared to be markedly lost in the colonic crypts upon LY411,575 treatment (Fig. 2*E*). These results indicated that LY411,575 inhibits Notch activation and promotes goblet cell differentiation but also strongly inhibits proliferation of IECs, leading to a poor regenerative response and a severe exacerbation of DSS-colitis.

LY411,575 promotes goblet cell differentiation but inhibits proliferation of IECs in vitro. Previous in vivo results suggested that Notch activation might play critical roles in both the differentiation and proliferation of IECs. We further examined the in vitro effect of LY411,575 upon human colonic epithelial cell lines LS174T and HT29. As shown by the immunoblot analysis, the endogenous expression of both NICD1 and Hes1 was completely inhibited within LS174T cells by LY411,575 treatment (Fig. 3*A*). Consistent with this, RT-PCR analysis showed a marked decrease in Hes1 mRNA expression with LY411,575, which was maintained for up to 72 h (Fig. 3*B*). These data confirmed that LY411,575 could directly inhibit the activation of Notch within IECs.

Under this condition, we examined whether LY411,575 could promote goblet cell differentiation in vitro. Quantitative RT-PCR analysis showed a significant increase in MUC2 mRNA expression with LY411,575 treatment in both LS174T and HT29 cells (Fig. 3*C*). Consistent with this, a marked induction of MUC2 protein expression was observed in both of the cell lines that were treated with LY411,575 (Fig. 3*D*, red signal), resulting in a significant increase in the MUC2-positive cell population (Fig. 3*E*). The Alcian blue staining also showed a marked increase in mucin-producing cells in both cell lines with LY411,575 (Fig. 3*F*, black arrow). However, LY411,575 appeared to inhibit the proliferation of both cell lines since the incorporation of BrdU was significantly downregulated by LY411,575 (Fig. 3*G*). These results collectively showed that LY411,575 could directly inhibit Notch activation in IECs, which might subsequently promote goblet cell differentiation but also inhibit cell proliferation.

Activation of Notch1 suppresses goblet cell phenotype, but upregulates PLA2G2A secretion in human IECs. To further analyze the function of Notch activation in IECs, we gen-

Fig. 2. Inhibition of Notch activation by LY411,575 exacerbates DSS-colitis by impairing epithelial regeneration. *A*: LY411,575 suppresses Hes1 expression but also promotes MUC2 expression in mice intestine. After oral administration of LY411,575 or vehicle alone for 5 consecutive days, the small intestinal tissues of mice were subjected to quantitative RT-PCR analysis. Results from 3 mice in each group. Error bars represent SD. $*P < 0.05$ on the Student's *t*-test. *B*: LY411,575 significantly exacerbated wasting disease caused by DSS. As described in MATERIALS AND METHODS, mice were separated into 4 groups, and the body weight of each mouse was monitored throughout the experimental period. Error bars represent SD. $*P < 0.05$ for the difference between mice that were DSS treated (DSS + VEC and DSS + LY) or not treated (VEC and LY). $**P < 0.05$ for the difference between DSS + VEC and DSS + LY mice on the Student's *t*-test. *C*: LY411,575 exacerbated epithelial injury of DSS-colitis. Intestinal tissues of mice shown in *B* were subjected to histological analysis. Blue staining with Alcian blue represents mucin production (original magnification ×400). *D*: LY411,575 had no significant effect on inflammation of DSS-colitis. Histological scoring of colonic tissues obtained from each mice group is shown. Error bars represent SD. $*P < 0.05$ on the Student's *t*-test. *E*: LY411,575 inhibited proliferation of IECs via downregulation of Notch activity. Colonic tissues of mice were subjected to immunohistochemical staining for Hes1 and Ki-67. A less inflamed region was chosen for analysis of DSS + LY mice because the most inflamed region showed complete loss of the epithelial layer. Note that IECs expressing Hes1 or Ki-67 were confined within a narrow region of the colonic crypt in mice treated with LY411,575 (LY and DSS + LY).

erated a subline of LS174T cells (Tet-On NICD1 cells), in which forced expression of NICD1 could be induced in a tetracycline- or DOX-dependent manner. Immunoblot analysis of Tet-On NICD1 cells showed a clear induction of NICD1 and a subsequent increase in Hes1, with DOX addition (Fig. 4*A*). Consistent with this, the reporter activity of Hes1p-Luc was significantly upregulated with the induction of NICD1 in Tet-On NICD1 cells, indicating that there was an upregulation of the transcriptional activity of the Hes1 gene (Fig. 4*B*). These results confirmed that Tet-On NICD1 cells could express the functional NICD1 protein with DOX addition.

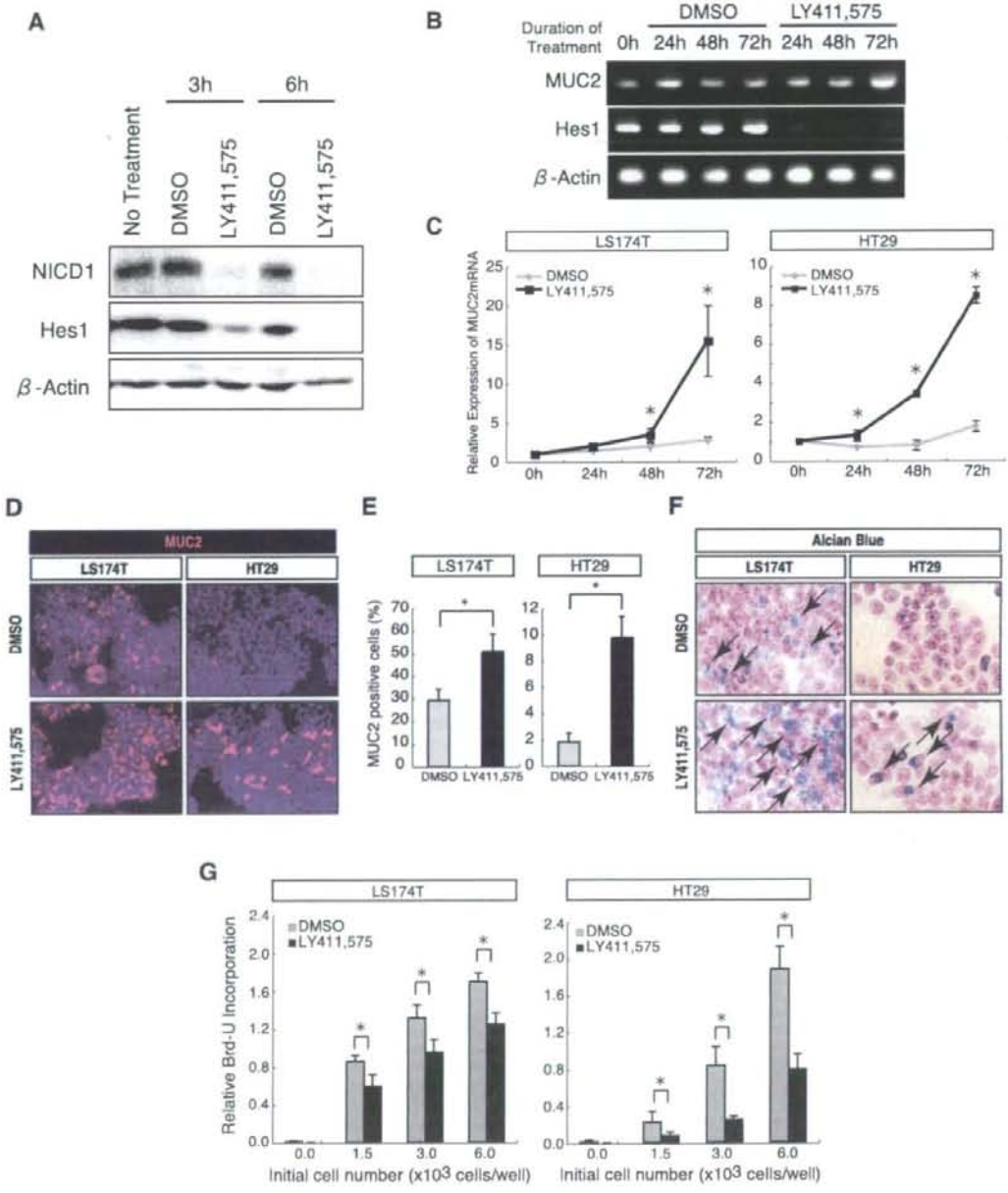

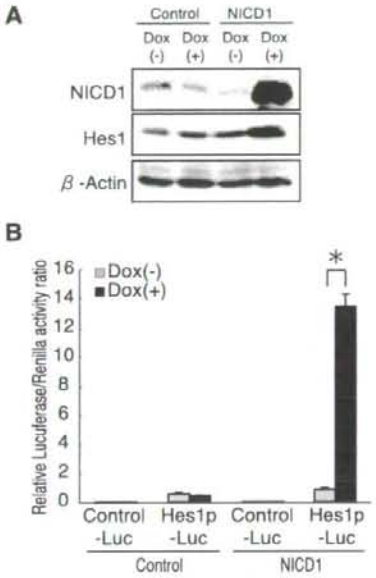

Fig. 4. Activation of Notch1 upregulates Hes1 expression in human IECs. *A*: establishment of a subline of LS174T cells expressing NICD1 under control of a tetracycline-dependent promoter (Tet-On NICD1 cells, designated as NICD1). Immunoblot analysis of Tet-On NICD1 cells showed a clear upregulation of both NICD1 and Hes1 expression with doxycycline (DOX) addition, whereas parental cells (designated as Control) remain unchanged. A low-sensitivity substrate (ECL) was used for visualization. *B*: transcriptional activity of Hes1 was upregulated with the expression of NICD1. Transcriptional activities of Hes1 gene in Tet-On NICD1 cells or control cells were analyzed by luciferase reporter assays using Hes1p-Luc. A reporter plasmid containing only the core-promoter of chicken β-actin gene served as a control (Control-Luc). Luciferase activities were measured after 12 h of culture with or without DOX. Error bars represent SD. $*P < 0.05$ on the Student's *t*-test.

Using this cell line, we found that the upregulation of NICD1 expression in LS174T cells significantly downregulated MUC2 mRNA expression (Fig. 5*A*). Further analysis with a microarray identified a group of genes that were up- or downregulated with NICD1 expression (Supplemental Tables 1 and 2). Among these genes, we focused on PLA2G2A, a gene expressed by Paneth cells, as it showed the most significant induction with NICD1 expression. Quantitative RT-PCR confirmed an upregulation of PLA2G2A mRNA expression with the NICD1 expression (Fig. 5*A*). Consistent with this, although the MUC2 protein expression was markedly suppressed (Fig. 5*B*), with resulting significant decreases in MUC2-positive cells (Fig. 5*C*) and mucin-producing cells (Fig. 5*D*), the PLA2G2A secretion was upregulated with NICD1 expression (Fig. 5*E*). These changes appeared to be regulated at the transcriptional level since the reporter activities of MUC2-Luc and PLA2-Luc showed a significant decrease and increase, respectively, with NICD1 expression (Fig. 5*F*). These results showed that, although the activation of Notch1 within LS174T cells suppressed goblet cell phenotype, it also upregulated the secretion of PLA2G2A, suggesting that the activation of Notch1 might surprisingly promote the acquisition of the specific functions of Paneth cells.

Notch1 is activated in crypt epithelial cells of the human intestine. Since we found that Notch signaling might regulate cell proliferation, goblet cell differentiation, and Paneth cell-specific function within IECs, we sought to clarify its relevance in human intestinal diseases. We first examined whether components of the Notch signaling pathway are expressed in the human intestine. An RT-PCR analysis of human intestinal tissues or epithelial cell lines successfully detected mRNAs of both Notch1 and Hes1 (Fig. 6*A*). The immunohistochemistry for NICD1 and Hes1 revealed that these proteins are expressed in the nuclei of crypt IECs (Fig. 6*B*). Similar to our observations in mice, the distribution of NICD1-positive or Hes1-positive IECs corresponded to that of Ki-67-positive IECs (Fig. 6*B*). Also, a magnified view of the staining showed a positive staining of NICD1 in columnar-shaped IECs and Paneth cells (Fig. 6*B*, black arrow) but not in goblet-shaped IECs (Fig. 6*B*, red arrowhead). Double staining of MUC2 and NICD1 confirmed the lack of NICD1 expression in goblet cells (Fig. 7*A*), whereas double staining of PLA2G2A and NICD1 confirmed expression of NICD1 in Paneth cells (Fig. 7B). These results strongly suggested that the NICD1 might function in vivo in the human intestine in a similar manner as was revealed in the in vitro study.

Increased activation of Notch1 is observed in the mucosa of UC. UC is one of the major forms of inflammatory bowel diseases, characterized by the persistent inflammation and ulcer formation in the colon. In the active region of UC, a loss of goblet cells, an ectopic expression of Paneth cell genes, and an increase in IEC proliferation are all known to be common pathological findings (7, 8, 13, 23). Thus our results strongly suggested that all of these pathological findings in UC might be mediated by the activation of Notch1 in IECs. We performed

Fig. 3. Inhibition of Notch activation promotes differentiation of goblet cells but suppresses proliferation of human IECs. *A*: LY411,575 downregulated expression of Notch1 intracellular domain (NICD1) and Hes1 in LS174T cells. Immunoblot analysis of LS174T cells treated with LY411,575 showing downregulation of endogenous NICD1 and Hes1 expression within 6 h from treatment. Cells treated with DMSO alone served as control. A high-sensitivity substrate (ECL Advance) was used for visualization. *B*: LY411,575 upregulated expression of MUC2 in LS174T cells. LS174T cells were subjected to semiquantitative RT-PCR analysis after treatment with either LY411,575 or DMSO. Note that expression of Hes1 was markedly decreased, whereas expression of MUC2 was increased after 72 h of treatment with LY411,575. *C*: LY411,575 significantly increased expression of MUC2 mRNA in both LS174T and HT29 cells. Cells were subjected to quantitative RT-PCR analysis after 0, 24, 48, and 72 h of treatment with either LY411,575 or DMSO. Error bars represent SD. $*P < 0.05$ for the difference between DMSO and LY411,575 treatment at the same time points on the Student's *t*-test. *D*: LY411,575 induced expression of MUC2 protein (red) in LS174T and HT29 cells. Cells were subjected to immunofluorescent staining of MUC2 after 72 h of treatment with either LY411,575 or DMSO (original magnification ×200). *E*: LY411,575 significantly increased the MUC2-positive cell populations among LS174T and HT29 cells. Quantitative analysis of *D* is shown by percent of MUC2-positive cells within total nucleated cells. Error bars represent SD. $*P < 0.05$, on the Student's *t*-test. *F*: LY411,575 induced mucin production in LS174T and HT29 cells. Cells were subjected to Alcian blue staining (black arrow) after 72 h of treatment with either LY411,575 or DMSO (original magnification ×400). *G*: LY411,575 significantly downregulated proliferation of LS174T and HT29 cells. A significant decrease in BrdU incorporation was observed with LY411,575 treatment in LS174T and HT29 cells. Incorporation of BrdU was measured by ELISA. Results are shown as arbitrary units of relative BrdU incorporation. Error bars represent SD. $*P < 0.05$ on the Student's *t*-test.

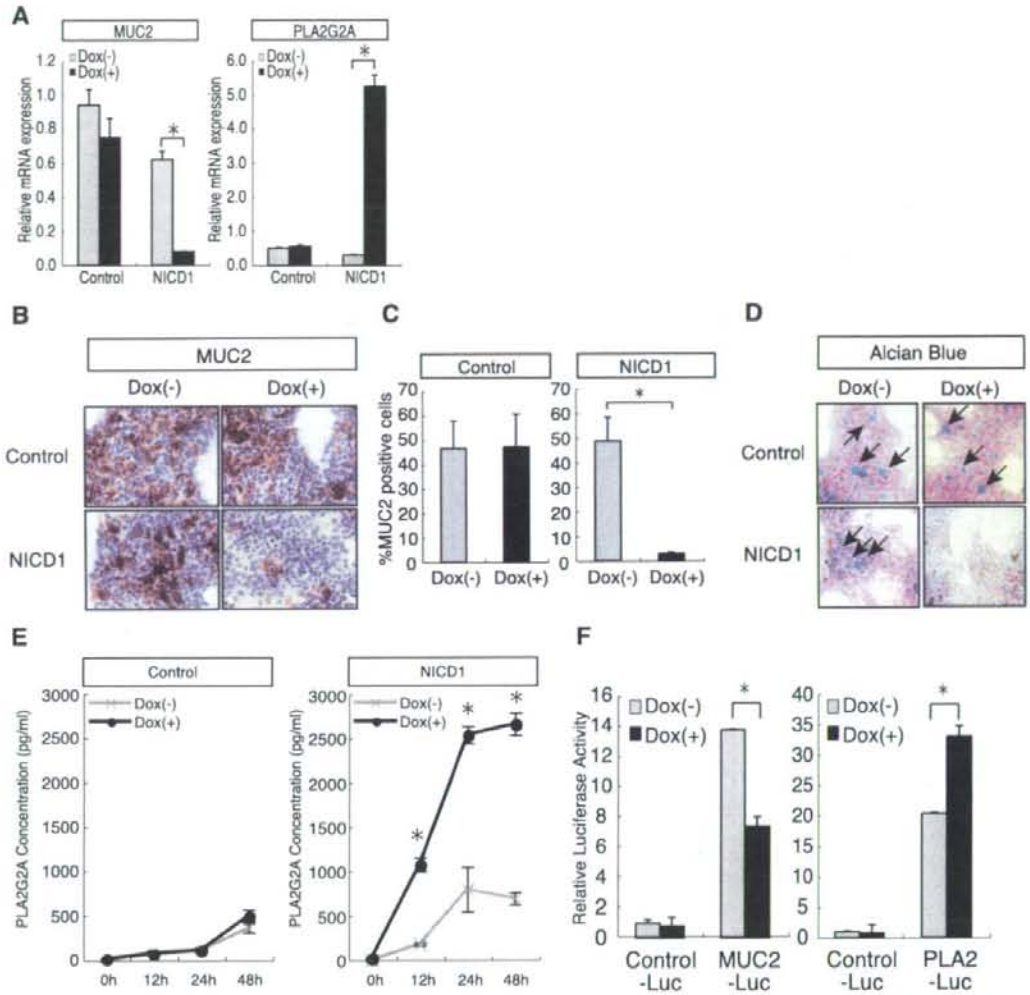

Fig. 5. Activation of Notch1 suppresses goblet cell differentiation but promotes expression of PLA2G2A of human IECs. *A*: expression of NICD1 in LS174T cells downregulated the expression of MUC2 but upregulated the expression of PLA2G2A. Quantitative RT-PCR analysis of MUC2 and PLA2G2A expression in Tet-On NICD1 cells and control cells is shown. Cells were subjected to analysis after 48 h of culture with or without DOX. Error bars represent SD. $*P < 0.05$ on the Student's *t*-test. *B*: expression of NICD1 in LS174T cells downregulated MUC2 protein expression. Tet-On NICD1 cells or control cells were subjected to immunostaining of MUC2 after 48 h of culture with or without DOX. Brown staining with DAB showed positive staining for MUC2 (original magnification ×200). *C*: expression of NICD1 in LS174T cells significantly reduced the number of cells expressing MUC2. Quantitative analysis of immunostaining shown in *B* is shown. Number of cells positively stained for MUC2 was counted and shown as percent of total nucleated cells. Error bars represent SD. $*P < 0.05$ on the Student's *t*-test. *D*: expression of NICD1 suppressed mucin production by LS174T cells. Tet-On NICD1 cells or control cells were treated as described in *B* and subjected to Alcian blue staining. The blue staining represents mucin-producing cells. (black arrow, original magnification ×800). *E*: expression of NICD1 upregulated PLA2G2A secretion of LS174T cells. Tet-On NICD1 cells or control cells were cultured with or without DOX, and culture supernatants collected at various time points were subjected to quantification of PLA2G2A using ELISA. Error bars represent SD. $*P < 0.05$ compared between DOX (+) and DOX (-) on the Student's *t*-test. *F*: expression of NICD1 in LS174T cells downregulated transcriptional activity of MUC2 gene but upregulated transcriptional activity of PLA2G2A gene. Transcriptional activity of MUC2 gene and PLA2G2A gene were measured by luciferase reporter assays using MUC2-Luc and PLA2-Luc as a reporter plasmid, respectively. pGL3-basic served as a control (Control-Luc). Luciferase activities in Tet-On NICD1 cells were analyzed after 12 h of culture with or without DOX. Error bars represent SD. $*P < 0.05$ on the Student's *t*-test.

histological analysis and found that in the crypts of UC, mucin production is markedly decreased (Fig. 8*A*, *top*, blue), whereas the number of Ki-67-expressing cells are markedly increased, distributing from the bottom to the uppermost part of the crypt (Fig. 8*A*, *bottom*, brown). In such crypts, NICD1-expressing cells showed the same distribution as Ki-67-expressing cells (Fig. 8*A*, *middle*, brown), suggesting that Notch1 is activated in an expanded proliferating cell population within the crypts of

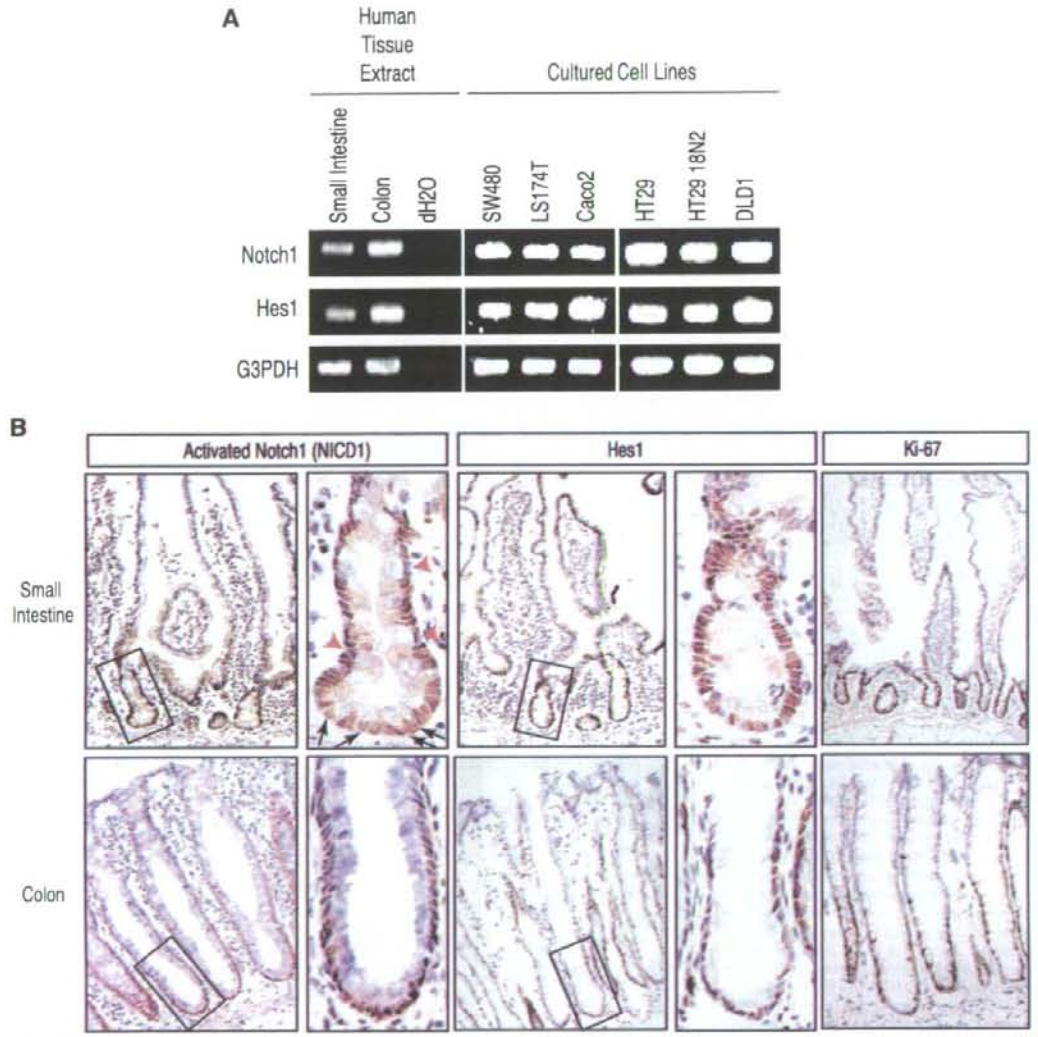

Fig. 6. Notch signaling is activated in crypt epithelial cells of the human intestine. *A*: RT-PCR analysis of human intestinal tissues and human intestinal epithelial cell lines. Expression of both Notch1 and Hes1 are clearly detected in all the examined tissues and cell lines. *B*: immunostaining of human intestinal tissues showing expression of NICD1, Hes1, and Ki-67. Brown staining with DAB showed positive results for NICD1, Hes1, and Ki-67 (original magnification ×200). Magnified view of the squared area is shown in the right side of the original picture (original magnification ×1000). Black arrows show Paneth cells clearly containing granules in the cytoplasm showing positive staining for NICD1, whereas red arrowheads show goblet-shaped cells lacking NICD1 staining.

UC. A quantitative analysis revealed that the number of IECs expressing NICD1 or Ki-67 per crypt is significantly increased, whereas the number of IECs producing mucin is significantly decreased in the crypts of UC (Fig. 8*B*).

We also looked for IECs expressing PLA2G2A within the colonic crypts. There was no expression of PLA2G2A in the crypts of the normal colon (Fig. 9*A*). However, an ectopic expression of PLA2G2A was clearly found in the crypts of the colon epithelia with UC (Fig. 9*B*). Our histological analysis revealed that Notch1 is clearly activated in such IECs ectopically expressing PLA2G2A (Fig. 9, *C* and *D*). Such activation of Notch1 in PLA2G2A-expressing cells could also be found in less inflamed regions of UC where there were fewer PLA2G2A-expressing IECs (Fig. 9, *E* and *F*).

From these results, we confirmed that Notch1 is activated in a greater number of crypt IECs in UC, presumably mediating goblet cell depletion, cell proliferation, and ectopic expression of PLA2G2A. We suggest that such Notch1-mediated changes

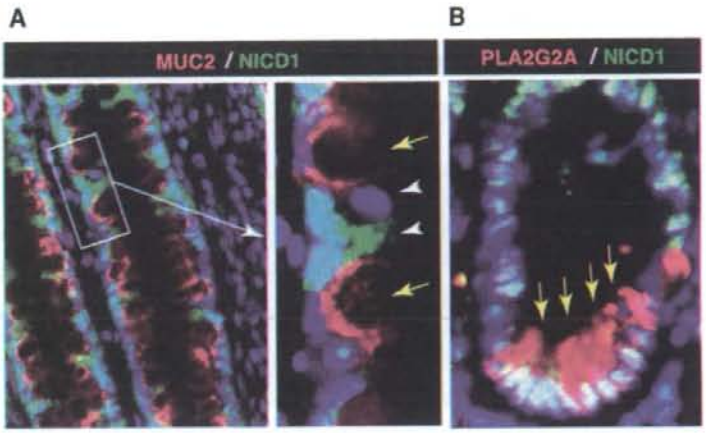

Fig. 7. Human Notch1 is not activated in IECs expressing MUC2 but is activated in IECs expressing PLA2G2A. *A*: human Notch1 was not activated in IECs expressing MUC2 in vivo. Double staining for MUC2 (red) and NICD1 (green) using human colonic tissue is shown. NICD1 and MUC2 were expressed in distinct populations of epithelial cells (*left*, ×400). A magnified view (*right*, ×1600) clearly shows cytoplasmic staining of MUC2 in goblet-shaped cells (yellow arrow), whereas nuclear staining of NICD1 in columnar-shaped cells (white arrowhead). *B*: human Notch1 is activated in IECs expressing PLA2G2A in vivo. Double staining for PLA2G2A (red) and NICD1 (green) using a human small intestinal tissue is shown. NICD1 and PLA2G2A were coexpressed in IECs residing at the lowest part of the crypt, suggesting activation of Notch1 in Paneth cells (yellow arrow, original magnification ×1000).

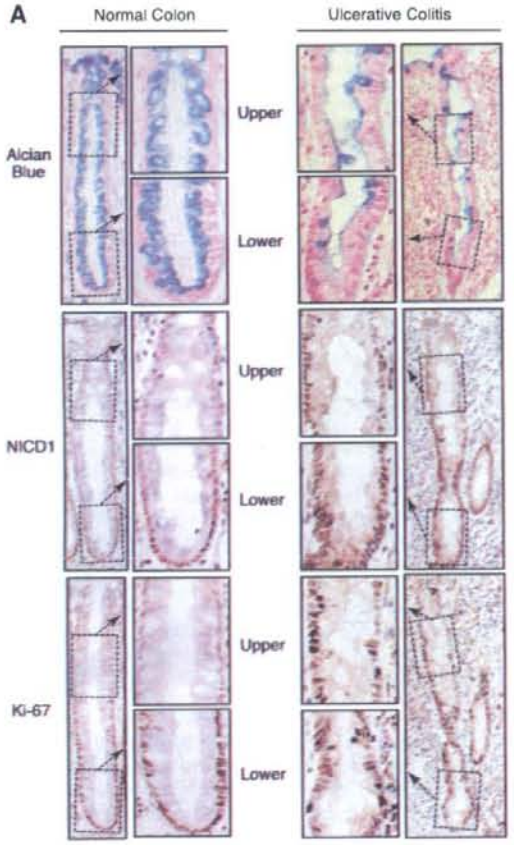

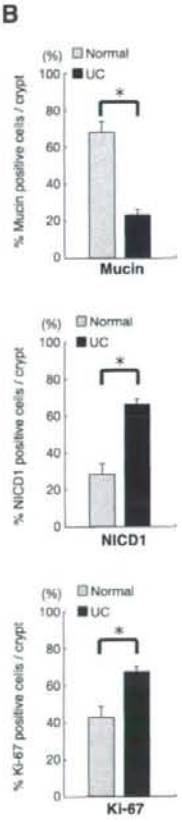

Fig. 8. Increased activation of Notch1 is observed in the crypts of patients with ulcerative colitis (UC). *A*: decreased expression of mucin and increased expression of both NICD1 and Ki-67 were observed in crypts of patients with UC. Mucin expression was examined by Alcian blue staining, whereas expression of NICD1 or Ki-67 was examined by immunohistochemistry with the use of human colonic tissues. Inner column shows magnified view of the upper (Upper) and lower (Lower) crypt areas identified by dashed line in the outer column. A marked decrease in Alcian blue-positive IECs is observed in a crypt of a patient with UC (*top*). In contrast, a marked increase in IECs expressing NICD1 (brown, *middle*) or Ki-67 (brown, *bottom*) was observed in patients with UC. Distribution of IECs expressing NICD1 or Ki-67 was restricted to the lower part of the crypt in normal colon, but it extended to the most upper region of the crypt in UC (original magnification, outer column ×400, inner column ×1600). *B*: significant decrease in IECs expressing mucin and significant increase in IECs expressing NICD1 or Ki-67 were observed in crypts of patients with UC. Quantitative analysis of the histological staining for mucin, NICD1, and Ki-67 is shown. Number of IECs positive for Alcian blue staining or immunohistochemical staining for NICD1 and Ki-67, respectively, were counted per crypt and normalized by total number of IECs. Results are shown as percent positive IECs per crypt. Error bars represent SD. $^*P < 0.05$ on the Student's *t*-test.

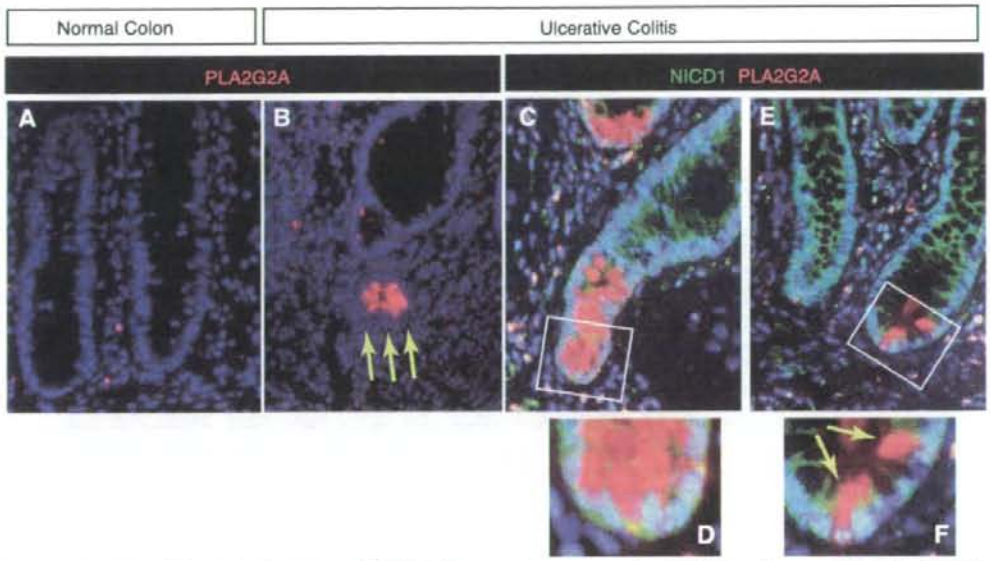

Fig. 9. Notch1 is activated in IECs ectopically expressing PLA2G2A. Fluorescent immunostaining for PLA2G2A (red) was completely negative in the crypts of normal colon (*A*, original magnification ×400), whereas some of the IECs in the crypts of a patient with UC were clearly positive for PLA2G2A (*B*, yellow arrow, original magnification ×400). Some cells in the lamina propria were also positive for PLA2G2A. Double immunostaining for NICD1 (green) and PLA2G2A (red) showed coexpression of NICD1 and PLA2G2A by colonic IECs of a patient with UC (*C–F*). In the inflamed region (*C, D*), NICD1 was expressed in most parts of the crypt IECs, and some proportion of those IECs coexpressed PLA2G2A (*C*, original magnification ×400). A magnified view (*D*, original magnification ×1000) of the indicated region (white square in *C*) clearly showed a nuclear distribution of NICD1 and a cytoplasmic distribution of PLA2G2A. In a less inflamed region, few IECs appeared to be positive for both NICD1 and PLA2G2A (*E*, original magnification ×400). Magnified view of the indicated region (white square in *E*) confirms coexpression of NICD1 and PLA2G2A in the nucleus and cytoplasm of an IEC, respectively (*F*, yellow arrow, original magnification ×1000).

observed in the mucosa of UC are not detrimental changes contributing to the persistence of the disease, but rather they are positive responses that help to regenerate the damaged epithelia, thereby aggressively contributing to the termination and recovery from the disease.

DISCUSSION

To date, several studies using knockout mice have revealed various functions of Notch signaling in IECs; one critical function is that of regulating the cell fates of IECs (31). The recent model accepted in such studies implicates Notch activation as a positive regulator of absorptive cell differentiation but a negative regulator of the differentiation of secretory lineage cells, including goblet cells. However, studies have suggested that Notch activation not only acts to determine the cell fates of progenitor IECs, but it may also regulate the number of proliferating populations within the crypt (6, 28, 33). Our results are consistent with the previous observations, and they further highlight the critical role of Notch activation in a situation when the rapid expansion of IECs is required (e.g., during the regeneration process in UC). Since the in vivo phenotype of Notch inhibition showed not only the loss of absorptive lineage cells but also the loss of the entire epithelial layer, this suggested that the activation of Notch may contribute to the expansion of both absorptive and secretory precursor cells and even stem cells. This is consistent with the observation by Vooijs et al. (34) that IECs that matured into absorptive cells must have also experienced Notch activation during development from the stem cell. Thus our results demonstrated the importance of Notch activation in the expansion of multilineage precursor IECs, whose function becomes critically required when tissue damage is present. In contrast, although Notch activation was predominant in the proliferating IECs of the colitic mucosa, its role in postmitotic IECs might be of less importance (42).

A recent study has shown that the chronic inhibition of Notch activation using LY411,575 (for up to 15 consecutive days) could impair the development of lymphoid cells (14, 36). Thus it may be possible that such an effect of LY411,575 might have altered the local immune function of the DSS-treated mice and thereby exacerbated their colitis. Indeed, LY411,575 proved to have a systemic effect, especially on the development of thymocytes (Supplemental Fig. S1). However, no effect was observed on splenocytes (Supplemental Fig. S1). Also, no effect was observed on local production of proinflammatory cytokines (Supplemental Fig. S2). Thus, although it is possible that LY411,575 might have some effect on the inflammatory response, its involvement on the exacerbation of the present colitis model may be minimal.

Also, GSI has been reported to promote the differentiation and inhibit proliferation of mice intestinal adenoma through the inhibition of Notch activation (33). Therefore, GSIs have been reported to have an antitumor effect (32). However, our results showed that the effects of GSIs may not be specific for tumor

cells. GSIs have almost the same effect on progenitor cells of the normal and regenerating crypt, which becomes critically toxic once the epithelia have been damaged. Thus caution is needed with the use of GSIs when intestinal tissue damage is present.

Although studies have revealed various extrinsic factors promoting the regeneration of the intestinal epithelia (2, 3), the intracellular mechanism mediating the regenerative process has not been fully elucidated (15). Our data show that Notch activation maintains the larger number of IECs in the immature state, thereby promoting the proliferation and supporting the rapid recovery of IECs needed to restore proper epithelial structure. Thus we identified Notch signaling as one of the main intracellular pathways mediating the organized regenerative response of the intestinal epithelia. Although we know that several ligands and receptors of the Notch pathway are expressed in the intestine (24, 26), we do not know the precise mechanism by which these ligands activate Notch receptors, in particular IECs. A recent study by Riccio et al. (22) clearly showed that both Notch1 and Notch2 function redundantly in the intestinal epithelia and that they directly regulate the cell cycle progression of crypt progenitor cells. Thus an analysis of the Notch ligand expression is needed to understand the mechanism by which these Notch receptors could be activated during epithelial regeneration and the mechanism by which such activation could be downregulated at the later stage of regeneration.

One of our surprising findings was the upregulation of PLA2G2A in Notch-activated IECs, suggesting that Notch might also modulate immune functions of IECs. PLA2G2A is usually expressed in Paneth cells, and it is known to have an antimicrobial effect (4). The loss of the continuity of the epithelial layer allows various and abundant microorganisms to invade the submucosal area, thereby promoting inflammation and further destruction of the mucosa. Thus the local secretion of PLA2G2A at the damaged mucosal area may be quite beneficial for limiting bacterial invasion and providing a proper environment for regeneration. However, previous reports have shown that PLA2G2A is also expressed by neutrophils and macrophages accumulating at the inflamed mucosa of colitis (29, 39). Consistent with this, we observed an infiltration of PLA2G2A-positive cells in the lamina propria of inflamed mucosa in UC (Fig. 9, *C–F*). An RT-PCR analysis of DSS-colitis showed a significant upregulation of PLA2G2A expression in the inflamed colonic mucosa (Supplemental Fig. S3). However, such an upregulation was not inhibited with LY411,575 treatment, suggesting that the expression of PLA2G2A by neutrophils or macrophages might be less dependent on Notch activation. In those cells, intracellular pathways such as NF-κB might function to promote expression of PLA2G2A in the inflamed colonic mucosa (37). Also, our histological analysis suggested that the upregulation of PLA2G2A secretion was not a general but a partial response in Notch-activated IECs, indicating that an additional condition is required for ectopic expression of PLA2G2A.

Our microarray analysis also revealed a number of genes other than PLA2G2A that are regulated by NICD1 in IECs. Although the results did not show an upregulation of other genes specific to Paneth cells such as lysozyme or α-defensins, our quantitative RT-PCR confirmed that genes such as clusterin or spermidine/spermine N1-acetyltransferase were also upregulated upon Notch1 activation in LS174T cells (data not shown). Trefoil factor-1 may also promote Notch-mediated tissue regeneration because it is known to be a key factor in restitution (11). The group of genes shown in the present analysis was quite distinct from the previous microarray analysis comparing GSI-treated and untreated intestinal tissues (14, 27). Because we used an in vitro IEC-based assay, the group of genes identified can be recognized as candidates of the IEC-specific target genes of Notch. However, because only a limited number of genes were analyzed (up to 10,000 annotated genes) in the present study, a further analysis including a larger group of genes may elucidate additional genes that are regulated downstream of Notch.

In conclusion, Notch signaling acts as an indispensable intracellular signaling pathway in IECs, especially during tissue regeneration. It regulates not only the differentiation, but also the proliferation of IECs, and it also regulates the immune function of IECs. We have shown for the first time that such functions of Notch are also present in the human intestine, both under normal conditions and when tissue damage has occurred. The present study provides a novel molecular basis for the advanced understanding of the regeneration process in the human intestinal epithelia, which may be utilized to establish alternative therapies for refractory ulcers caused by various intestinal diseases.

ACKNOWLEDGMENTS

The authors thank Dr. Tetsuo Sudo for providing the Hes1 antibody, Drs. Ryoichiro Kageyama and Yasuhito Yuasa for providing the plasmids, Drs. Hisao Fukushima, Kazutaka Koganei, Kenichi Sugihara, and Hiroyuki Uetake for providing the tissue samples, Drs. Hideyuki Okano and Takaaki Ito for the helpful discussion, and Dr. Hisanobu Kawamura, Dr. Michio Onizawa, and Ms. Motomi Yamazaki for technical assistance.

GRANTS

This study was supported in part by grants-in-aid for Scientific Research, Scientific Research on Priority Areas, Exploratory Research, and Creative Scientific Research from the Japanese Ministry of Education, Culture, Sports, Science and Technology, The Japanese Ministry of Health, Labor and Welfare, The Japanese Society of Gastroenterology, The Foundation for Advancement of International Science, Research Fund of Mitsukoshi Health and Welfare Foundation, and the Research Fund of Japan Intractable Diseases Research Foundation.

REFERENCES

1. **Bjerknes M, Cheng H.** Gastrointestinal stem cells. II. Intestinal stem cells. *Am J Physiol Gastrointest Liver Physiol* 289: G381–G387, 2005.
2. **Bjerknes M, Cheng H.** Modulation of specific intestinal epithelial progenitors by enteric neurons. *Proc Natl Acad Sci USA* 98: 12497–12502, 2001.
3. **Brauchle M, Madlener M, Wagner AD, Angermeyer K, Lauer U, Hofschneider PH, Gregor M, Werner S.** Keratinocyte growth factor is highly overexpressed in inflammatory bowel disease. *Am J Pathol* 149: 521–529, 1996.
4. **Buckland AG, Wilton DC.** The antibacterial properties of secreted phospholipases A(2). *Biochim Biophys Acta* 1488: 71–82, 2000.
5. **Fahlgren A, Hammarstrom S, Danielsson A, Hammarstrom ML.** Increased expression of antimicrobial peptides and lysozyme in colonic epithelial cells of patients with ulcerative colitis. *Clin Exp Immunol* 131: 90–101, 2003.
6. **Fre S, Huyghe M, Mourikis P, Robine S, Louvard D, Artavanis-Tsakonas S.** Notch signals control the fate of immature progenitor cells in the intestine. *Nature* 435: 964–968, 2005.
7. **Haapamaki MM, Gronroos JM, Nurmi H, Alanen K, Kallajoki M, Nevalainen TJ.** Gene expression of group II phospholipase A2 in intestine in ulcerative colitis. *Gut* 40: 95–101, 1997.
8. **Haapamaki MM, Gronroos JM, Nurmi H, Irjala K, Alanen KA, Nevalainen TJ.** Phospholipase A2 in serum and colonic mucosa in ulcerative colitis. *Scand J Clin Lab Invest* 59: 279–287, 1999.

9. **Jensen J, Pedersen EE, Galante P, Hald J, Heller RS, Ishibashi M, Kageyama R, Guillemot F, Serup P, Madsen OD.** Control of endodermal endocrine development by Hes-1. *Nat Genet* 24: 36–44, 2000.
10. **Kopan R.** Notch: a membrane-bound transcription factor. *J Cell Sci* 115: 1095–1097, 2002.
11. **Longman RJ, Douthwaite J, Sylvester PA, Poulsom R, Corfield AP, Thomas MG, Wright NA.** Coordinated localisation of mucins and trefoil peptides in the ulcer associated cell lineage and the gastrointestinal mucosa. *Gut* 47: 792–800, 2000.
12. **Matsumoto T, Okamoto R, Yajima T, Mori T, Okamoto S, Ikeda Y, Mukai M, Yamazaki M, Oshima S, Tsuchiya K, Nakamura T, Kanai T, Okano H, Inazawa J, Hibi T, Watanabe M.** Increase of bone marrow-derived secretory lineage epithelial cells during regeneration in the human intestine. *Gastroenterology* 128: 1851–1867, 2005.
13. **McCormick DA, Horton LW, Mee AS.** Mucin depletion in inflammatory bowel disease. *J Clin Pathol* 43: 143–146, 1990.
14. **Milano J, McKay J, Dagenais C, Foster-Brown L, Pognan F, Gadient R, Jacobs RT, Zacco A, Greenberg B, Ciaccio PJ.** Modulation of notch processing by gamma-secretase inhibitors causes intestinal goblet cell metaplasia and induction of genes known to specify gut secretory lineage differentiation. *Toxicol Sci* 82: 341–358, 2004.
15. **Okamoto R, Watanabe M.** Cellular and molecular mechanisms of the epithelial repair in IBD. *Dig Dis Sci*, 50 *Suppl* 1: S34–S38, 2005.
16. **Okamoto R, Watanabe M.** Molecular and clinical basis for the regeneration of human gastrointestinal epithelia. *J Gastroenterol* 39: 1–6, 2004.
17. **Okayasu I, Hatakeyama S, Yamada M, Ohkusa T, Inagaki Y, Nakaya R.** A novel method in the induction of reliable experimental acute and chronic ulcerative colitis in mice. *Gastroenterology* 98: 694–702, 1990.
18. **Oshima S, Nakamura T, Namiki S, Okada E, Tsuchiya K, Okamoto R, Yamazaki M, Yokota T, Aida M, Yamaguchi Y, Kanai T, Handa H, Watanabe M.** Interferon regulatory factor 1 (IRF-1) and IRF-2 distinctively upregulate gene expression and production of interleukin-7 in human intestinal epithelial cells. *Mol Cell Biol* 24: 6298–6310, 2004.
19. **Podolsky DK.** Healing the epithelium: solving the problem from two sides. *J Gastroenterol* 32: 122–126, 1997.
20. **Radtke F, Clevers H, Riccio O.** From gut homeostasis to cancer. *Curr Mol Med* 6: 275–289, 2006.
21. **Rakoff-Nahoum S, Paglino J, Eslami-Varzaneh F, Edberg S, Medzhitov R.** Recognition of commensal microflora by toll-like receptors is required for intestinal homeostasis. *Cell* 118: 229–241, 2004.
22. **Riccio O, van Gijn ME, Bezdek AC, Pellegrinet L, van Es JH, Zimber-Strobl U, Strobl LJ, Honjo T, Clevers H, Radtke F.** Loss of intestinal crypt progenitor cells owing to inactivation of both Notch1 and Notch2 is accompanied by derepression of CDK inhibitors p27Kip1 and p57Kip2. *EMBO Rep* 9: 377–383, 2008.
23. **Riddle RH.** *Pathology of Idiopathic Inflammatory Bowel Disease*. Orlando, FL: Saunders, 2004.
24. **Sander GR, Powell BC.** Expression of notch receptors and ligands in the adult gut. *J Histochem Cytochem* 52: 509–516, 2004.
25. **Sasai Y, Kageyama R, Tagawa Y, Shigemoto R, Nakanishi S.** Two mammalian helix-loop-helix factors structurally related to Drosophila hairy and Enhancer of split. *Genes Dev* 6: 2620–2634, 1992.
26. **Schroder N, Gossler A.** Expression of Notch pathway components in fetal and adult mouse small intestine. *Gene Expr Patterns* 2: 247–250, 2002.
27. **Searfoss GH, Jordan WH, Calligaro DO, Galbreath EJ, Schirtzinger LM, Berridge BR, Gao H, Higgins MA, May PC, Ryan TP.** Adipsin, a biomarker of gastrointestinal toxicity mediated by a functional gamma-secretase inhibitor. *J Biol Chem* 278: 46107–46116, 2003.
28. **Stanger BZ, Datar R, Murtaugh LC, Melton DA.** Direct regulation of intestinal fate by Notch. *Proc Natl Acad Sci USA* 102: 12443–12448, 2005.
29. **Tomita Y, Jyoyama H, Kobayashi M, Kuwabara K, Furue S, Ueno M, Yamada K, Ono T, Teshirogi I, Nomura K, Arita H, Okayasu I, Hori Y.** Role of group IIA phospholipase A2 in rat colitis induced by dextran sulfate sodium. *Eur J Pharmacol* 472: 147–158, 2003.
30. **Tsuchiya K, Nakamura T, Okamoto R, Kanai T, Watanabe M.** Reciprocal targeting of Hath1 and beta-catenin by Wnt glycogen synthase kinase 3beta in human colon cancer. *Gastroenterology* 132: 208–220, 2007.
31. **van Den Brink GR, de Santa Barbara P, Roberts Development DJ.** Epithelial cell differentiation—a Mather of choice. *Science* 294: 2115–2116, 2001.
32. **van Es JH, Clevers H.** Notch and Wnt inhibitors as potential new drugs for intestinal neoplastic disease. *Trends Mol Med* 11: 496–502, 2005.
33. **van Es JH, van Gijn ME, Riccio O, van den Born M, Vooijs M, Begthel H, Cozijnsen M, Robine S, Winton DJ, Radtke F, Clevers H.** Notch/gamma-secretase inhibition turns proliferative cells in intestinal crypts and adenomas into goblet cells. *Nature* 435: 959–963, 2005.
34. **Vooijs M, Ong CT, Hadland B, Huppert S, Liu Z, Korving J, van den Born M, Stappenbeck T, Wu Y, Clevers H, Kopan R.** Mapping the consequence of Notch1 proteolysis in vivo with NIP-CRE. *Development* 134: 535–544, 2007.
35. **Watanabe M, Ueno Y, Yajima T, Okamoto S, Hayashi T, Yamazaki M, Iwao Y, Ishii H, Habu S, Uehira M, Nishimoto H, Ishikawa H, Hata J, Hibi T.** Interleukin 7 transgenic mice develop chronic colitis with decreased interleukin 7 protein accumulation in the colonic mucosa. *J Exp Med* 187: 389–402, 1998.
36. **Wong GT, Manfra D, Poulet FM, Zhang Q, Josien H, Bara T, Engstrom L, Pinzon-Ortiz M, Fine JS, Lee HJ, Zhang L, Higgins GA, Parker EM.** Chronic treatment with the gamma-secretase inhibitor LY-411,575 inhibits beta-amyloid peptide production and alters lymphopoiesis and intestinal cell differentiation. *J Biol Chem* 279: 12876–12882, 2004.
37. **Wu F, Chakravarti S.** Differential expression of inflammatory and fibrogenic genes and their regulation by NF-kappaB inhibition in a mouse model of chronic colitis. *J Immunol* 179: 6988–7000, 2007.
38. **Wu J, Tung JS, Thorsett ED, Pleiss MA, Nissen JS, Neitz J, Latimer JH, John V, Freedman S,** inventors. Cycloalkyl, Lactam, Lactone and related compounds as β-amyloid peptide release inhibitors. US patent WO-1998028268, February 7, 1998.
39. **Yamaguchi O, Sugimura K, Ishizuka K, Suzuki K, Hasegawa K, Ohtsuka K, Honma T, Asakura H.** Correlation between serum phospholipase A(2) IIA levels and histological activity in patients with ulcerative colitis. *Int J Colorectal Dis* 17: 311–316, 2002.
40. **Yamamoto H, Bai YQ, Yuasa Y.** Homeodomain protein CDX2 regulates goblet-specific MUC2 gene expression. *Biochem Biophys Res Commun* 300: 813–818, 2003.
41. **Yamazaki M, Yajima T, Tanabe M, Fukui K, Okada E, Okamoto R, Oshima S, Nakamura T, Kanai T, Uehira M, Takeuchi T, Ishikawa H, Hibi T, Watanabe M.** Mucosal T cells expressing high levels of IL-7 receptor are potential targets for treatment of chronic colitis. *J Immunol* 171: 1556–1563, 2003.
42. **Zecchini V, Domaschenz R, Winton D, Jones P.** Notch signaling regulates the differentiation of post-mitotic intestinal epithelial cells. *Genes Dev* 19: 1686–1691, 2005.

The Journal of Immunology

MyD88-Dependent Pathway in T Cells Directly Modulates the Expansion of Colitogenic CD4$^+$ T Cells in Chronic Colitis[1]

Takayuki Tomita,* Takanori Kanai,[2]* Toshimitsu Fujii,* Yasuhiro Nemoto,* Ryuichi Okamoto,* Kiichiro Tsuchiya,* Teruji Totsuka,* Naoya Sakamoto,* Shizuo Akira,[†] and Mamoru Watanabe*

TLRs that mediate the recognition of pathogen-associated molecular patterns are widely expressed on/in cells of the innate immune system. However, recent findings demonstrate that certain TLRs are also expressed in conventional TCR$\alpha\beta^+$ T cells that are critically involved in the acquired immune system, suggesting that TLR ligands can directly modulate T cell function in addition to various innate immune cells. In this study, we report that in a murine model of chronic colitis induced in RAG-2$^{-/-}$ mice by adoptive transfer of CD4$^+$CD45RB^{high} T cells, both CD4$^+$CD45RB^{high} donor cells and the expanding colitogenic lamina propria CD4$^+$CD44^{high} memory cells expresses a wide variety of TLRs along with MyD88, a key adaptor molecule required for signal transduction through TLRs. Although RAG-2$^{-/-}$ mice transferred with MyD88$^{-/-}$CD4$^+$CD45RB^{high} cells developed colitis, the severity was reduced with the delayed kinetics of clinical course, and the expansion of colitogenic CD4$^+$ T cells was significantly impaired as compared with control mice transferred with MyD88$^{+/+}$CD4$^+$CD45RB^{high} cells. When RAG-2$^{-/-}$ mice were transferred with the same number of MyD88$^{+/+}$ (Ly5.1$^+$) and MyD88$^{-/-}$ (Ly5.2$^+$) CD4$^+$CD45RB^{high} cells, MyD88$^{-/-}$CD4$^+$ T cells showed significantly lower proliferative responses assessed by in vivo CFSE division assay, and also lower expression of antiapoptotic Bcl-2/Bcl-x$_L$ molecules and less production of IFN-γ and IL-17, compared with the paired MyD88$^{+/+}$CD4$^+$ T cells. Collectively, the MyD88-dependent pathway that controls TLR signaling in T cells may directly promote the proliferation and survival of colitogenic CD4$^+$ T cells to sustain chronic colitis. ***The Journal of Immunology*****, 2008, 180: 5291–5299.**

Inflammatory bowel diseases (IBD)[3] are caused by excessive tissue damaging by chronic inflammatory responses in the gut wall, and commonly take persistent courses (1, 2). According to the present understanding, the diseases are caused by infiltrated colitogenic effector/memory CD4$^+$ T cells within the inflamed mucosa, which are presumably primed by commensal Ag-loading dendritic cells (DCs) in lymphoid tissues (3). However, the nature of colitogenic CD4$^+$ T cells over time during chronic colitis under the persistent presence of commensal bacteria remains largely unknown.

Importantly, it is well-known that experimental colitis does not develop when mice are kept in a germfree condition (4–6), suggesting that intestinal microflora are essential to initiate and maintain colitogenic CD4$^+$ T cells by stimuli through 1) TCR signaling by one or more commensal Ags (signal 1) and 2) TLR signaling by pathogen-associated molecular patterns (PAMPs) in addition to cytokines (signal 3) and costimulatory signaling (signal 2) (7, 8). However, there are no reports showing that TLR signaling directly stimulates colitogenic CD4$^+$ T cells for their proliferation and/or survival.

It is widely recognized that TLRs are expressed in/on the innate immune cells (9, 10), such as macrophages, DCs, and epithelial cells, and are crucially important primarily to activate these professional and nonprofessional APCs and secondarily promote T cell responses (11). However, accumulating evidence has shown that certain TLRs are also expressed on/in TCR$\alpha\beta^+$ T cells that are major acquired immune cell populations (12), suggesting that TLR signaling may possibly have some direct function on adaptive immunity. Hence, to assess the direct role of TLR signaling initiated by PAMPs of commensal bacteria in modulation of colitogenic CD4$^+$ T cell expansion during the development and the persistence of chronic colitis, we performed a series of adoptive transfer colitis experiments by transfer of CD4$^+$CD45RB^{high} T cells that are deficient for MyD88, a key adaptor molecule of TLR signaling (13, 14), into RAG-2$^{-/-}$ recipient mice whose TLR pathways remained intact throughout the innate immune system.

Materials and Methods

Animals

Six- to 10-wk-old Ly5.2-background (Ly5.2$^+$) MyD88$^{-/-}$ mice (13) were used. Ly5.2$^+$ C57BL/6 mice were purchased from Japan Clea. Ly5.1-background C57BL/6 mice and Ly5.2$^+$ C57BL/6 RAG-2$^{-/-}$ mice were obtained from Taconic Farms and Central Laboratories for Experimental Animals (Kawasaki, Japan). Mice were maintained under specific pathogen-free conditions in the Animal Care Facility of Tokyo Medical and Dental University (Tokyo, Japan). All experiments were approved by the

*Department of Gastroenterology and Hepatology, Graduate School, Tokyo Medical and Dental University, Tokyo, Japan; and [†]Department of Host Defense, Research Institute for Microbial Diseases, Osaka University, Osaka, Japan

Received for publication July 26, 2007. Accepted for publication February 16, 2008.

The costs of publication of this article were defrayed in part by the payment of page charges. This article must therefore be hereby marked *advertisement* in accordance with 18 U.S.C. Section 1734 solely to indicate this fact.

[1] This work was supported in part by Grants-in-Aid for Scientific Research, Scientific Research on Priority Areas, Exploratory Research and Creative Scientific Research from the Japanese Ministry of Education, Culture, Sports, Science, and Technology; the Japanese Ministry of Health, Labor, and Welfare; the Japan Medical Association; and Foundation for Advancement of International Science.

[2] Address correspondence and reprint requests to Dr. Takanori Kanai, Department of Gastroenterology and Hepatology, Graduate School, Tokyo Medical and Dental University, 1-5-45 Yushima, Bunkyo-ku, Tokyo 113-8519, Japan. E-mail address: taka.gast@tmd.ac.jp

[3] Abbreviations used in this paper: IBD, inflammatory bowel disease; DC, dendritic cell; PAMP, pathogen-associated molecular pattern; PB, peripheral blood; SP, spleen; MLN, mesenteric lymph node; BM, bone marrow; WT, wild type; LP, lamina propria; IEL, intraepithelial cell; HPF, high-power field.

regional animal study committees and were done according to institutional guidelines and Home Office regulations.

Purification of T cell subsets

For isolation of peripheral blood (PB) lymphocytes, 600 μl of PB was collected from each mouse and was diluted 1/1 with PBS. The diluted PB was layered over Lymphosepar II (IBL) and centrifuged at 400 × *g* for 30 min at room temperature. Lymphocytes were then isolated from the plasma-Ficoll interface. Spleen (SP) and mesenteric lymph nodes (MLN) were mechanically disrupted into single-cell suspensions. Bone marrow (BM) was collected from the femur by flushing with sterile PBS.

$CD4^+$ T cells were isolated from SP cells of $MyD88^{-/-}$ and littermate $MyD88^{+/+}$ mice using the anti-CD4 (L3T4)-MACS system (Miltenyi Biotec) according to the manufacturer's instruction. Enriched $CD4^+$ T cells (94–96% pure, as estimated by FACSCalibur; BD Biosciences) were then labeled with PE-conjugated anti-mouse CD4 (RM4-5; BD Pharmingen) and FITC-conjugated anti-CD45RB (16A; BD Pharmingen). The subpopulation of $CD4^+CD45RB^{high}$ cells was collected by two-color sorting on a FACS Aria (BD Biosciences), and was >98.0% pure on reanalysis.

To obtain LP $CD4^+$ T cells, colitis was induced in $RAG\text{-}2^{-/-}$ mice by adoptive transfer of $CD4^+CD45RB^{high}$ T cells either from $MyD88^{-/-}$ or from littermate wild-type (WT) $MyD88^{+/+}$ mice as described previously (15). Colitic $CD4^+CD45RB^{high}$ T cell-transferred $RAG\text{-}2^{-/-}$ mice were sacrificed at 6–10 wk after transfer. The entire colon was opened longitudinally, washed with PBS, and cut into small pieces. The dissected mucosa was incubated with Ca^{2+}, Mg^{2+}-free HBSS containing 1 mM DTT (Sigma-Aldrich) for 45 min to remove mucus and then treated with 2.0 mg/ml collagenase (Roche) and 0.01% DNase (Worthington Biomedical) for 2 h. The cells were pelleted twice through a 40% isotonic Percoll solution, and then subjected to Ficoll-Hypaque density gradient centrifugation (40%/75%). Enriched lamina propria (LP) $CD4^+$ T cells were obtained by positive selection using anti-CD4 (L3T4) MACS magnetic beads. The resultant cells contained >95% $CD4^+$ cells when analyzed by FACSCalibur. To assess the expression of TLRs and MyD88 in $CD4^+$ T cells using RT-PCR, every cell population was isolated by FACS Aria (BD Biosciences) to gain >98% $CD4^+$ purity.

RT-PCR

Total RNA was isolated by using Isogen reagent (Nippon Gene). Aliquots of total RNA (0.5 μg) were used for cDNA synthesis in a 20-μl reaction volume using random primers. One microliter of reverse transcription product was amplified with 0.25 U of rTaq DNA polymerase (Toyobo) in a 25-μl reaction. Sense and antisense primers and the cycle numbers for the amplification of each gene (16) were as follows: TLR1, sense 5′-TCTCTGAAGGCTTTGTCGATACA-3′ and antisense 5′-GACAGAGCCTGTAAGCATATTCG-3′ (35 cycles); TLR2, sense 5′-TCTAAAGTCGATCCGCGACAT-3′ and antisense 5′-TACCCAGCTCGCTCACTACGT-3′ (35 cycles); TLR3, sense 5′-TTGTCTTCTGCACGAACCTG-3′ and antisense 5′-CGCAACGCAAGGATTTTATT-3′ (35 cycles); TLR4, sense 5′-CAAGAACATAGATCTGAGCTTCAACCC-3′ and antisense 5′-GCTGTCCAATAGGGAAGCTTTCTAGAG-3′ (35 cycles); TLR5, sense 5′-ACTGAATTCCTTAAGCGACGTA-3′ and antisense 5′-AGAAGATAAAGCCGTGCGAAA-3′ (35 cycles); TLR6, sense 5′-AACAGGATACGGAGCCTTGA-3′ and antisense 5′-CCAGGAAAGTCAGCTTCGTC-3′ (35 cycles); TLR7, sense 5′-TTCCGATACGATGAATATGCACG-3′ and antisense 5′-TGAGTTTGTCCAGAAGCCGTAAT-3′ (35 cycles); TLR8, sense 5′-GGCACAACTCCCTTGTGATT-3′ and antisense 5′-CATTTGGGTGCTGTTGTTTG-3′ (35 cycles); TLR9, sense 5′-CCGCAAGACTCTATTTGTGCTGG-3′ and antisense 5′-TGTCCCTAGTCAGGGCTGTACTCAG-3′ (35 cycles); MyD88, sense 5′-GGCCTTGTTAGACCGTGAGG-3′ and antisense 5′-TCATCTTCCCCTCTGCCCTA-3′ for (35 cycles); β-actin, sense 5′-GTGGGCCGCTCTAGGCACCAA-3′ and antisense 5′-CTCTTTGATGTCACGCACGATTTC-3′ (30 cycles). PCR products were separated on 1.8% agarose gels, stained with ethidium bromide, and visualized with a Lumi-Imager F1 (Roche Diagnostics).

Quantitative PCR

To validate gene expression changes, quantitative RT-PCR analysis was performed by Applied Biosystems 7500 using validated TaqMan Gene Expression Assays (Applied Biosystems). The TaqMan probes and primers for mouse Bcl-2 (assay identification number Mm00477631_m1) and mouse Bcl-x_L (assay identification number Mm00437783_m1) were Assay-on-Demand gene expression products (Applied Biosystems). The mouse β-actin gene was used as endogenous control (catalog number 4352933E; Applied Biosystems). The thermal cycler conditions were as follows: hold for 10 min at 95°C, followed a cycle of 95°C for 15 s and 60°C for 1 min for 45 cycles. All samples were performed in triplicate.

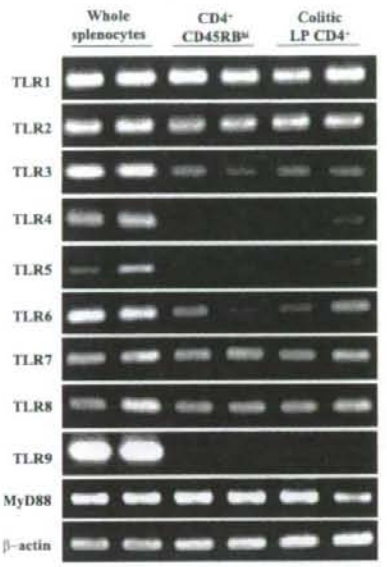

FIGURE 1. $CD4^+CD45RB^{high}$ donor cells and colitic LP $CD4^+$ T cells express mRNAs for TLR and MyD88. Splenocytes and $CD4^+CD45RB^{high}$ T cells from normal C57BL/6 mice, or LP $CD4^+$ T cells from colitic $RAG\text{-}2^{-/-}$ mice transferred with $CD4^+CD45RB^{high}$ T cells, were strictly isolated using FACSAria (purity, >98.0%) and subjected for total RNA extraction. The RNA was reverse transcripted and amplified with gene for specific primers. PCR products were separated by agarose gel electrophoresis and stained with ethidium bromide. All the RT-PCR experiments were performed at least three times on independent samples.

Amplification data were analyzed with an Applied Biosystems Sequence Detection Software version 1.3. The relative expression of the gene of interest was normalized by the expression of β-actin.

In vivo experimental design

We performed a series of in vivo transfer experiments to investigate the role of TLR signaling in $CD4^+CD45RB^{high}$ T cells or in colitogenic LP $CD4^+$ T cells in the development and persistence of murine chronic colitis.

Experiment 1. To assess the requirement of MyD88-dependent signaling in the development of colitis including the processes for T cell priming and activation, along with the persistence of colitogenic effector or memory $CD4^+$ T cells, we performed a cell transfer experiment using $MyD88^{-/-}$ and littermate WT $MyD88^{+/+}$ mice as donors. $CD4^+CD45RB^{high}$ T cells from $MyD88^{-/-}$ ($n = 6$) or $MyD88^{+/+}$ ($n = 6$) donors were injected i.p. into $RAG\text{-}2^{-/-}$ mice and the recipients were monitored for 4–6 wk after transfer. In another set of experiment using the present protocol, we monitored the groups of mice (each $n = 5$) to 10 wk after transfer to assess the kinetics of the development.

Experiment 2. To further assess the necessity of MyD88-dependent signaling in the development of colitis, we performed in vivo competition experiments. The same number (2.5×10^5 cells/mouse) of $CD4^+CD45RB^{high}$ T cells from $MyD88^{+/+}$ (Ly5.1$^+$) or $MyD88^{-/-}$ (Ly5.2$^+$) mice were coinjected i.p. into $RAG\text{-}2^{-/-}$ mice ($n = 6$), and the recipients were monitored for 6 wk after transfer.

Experiment 3. To assess the requirement of MyD88-dependent signaling for the persistence of colitogenic memory $CD4^+$ T cells in this $CD4^+CD45RB^{high}$ T cell-transferred colitis model, independently from the impact of naive T cell priming, activation, and differentiation, we performed the adoptive retransfer of colitogenic LP memory $CD4^+$ T cells derived from colitic mice that were transferred with $CD4^+CD45RB^{high}$ T cells of either $MyD88^{+/+}$ ($n = 6$) or $MyD88^{-/-}$ mice ($n = 6$) after 10 wk from transfer (17).

Experiment 4. To further assess the requirement of MyD88-dependent signaling for the persistence of colitogenic memory $CD4^+$ T cells, we

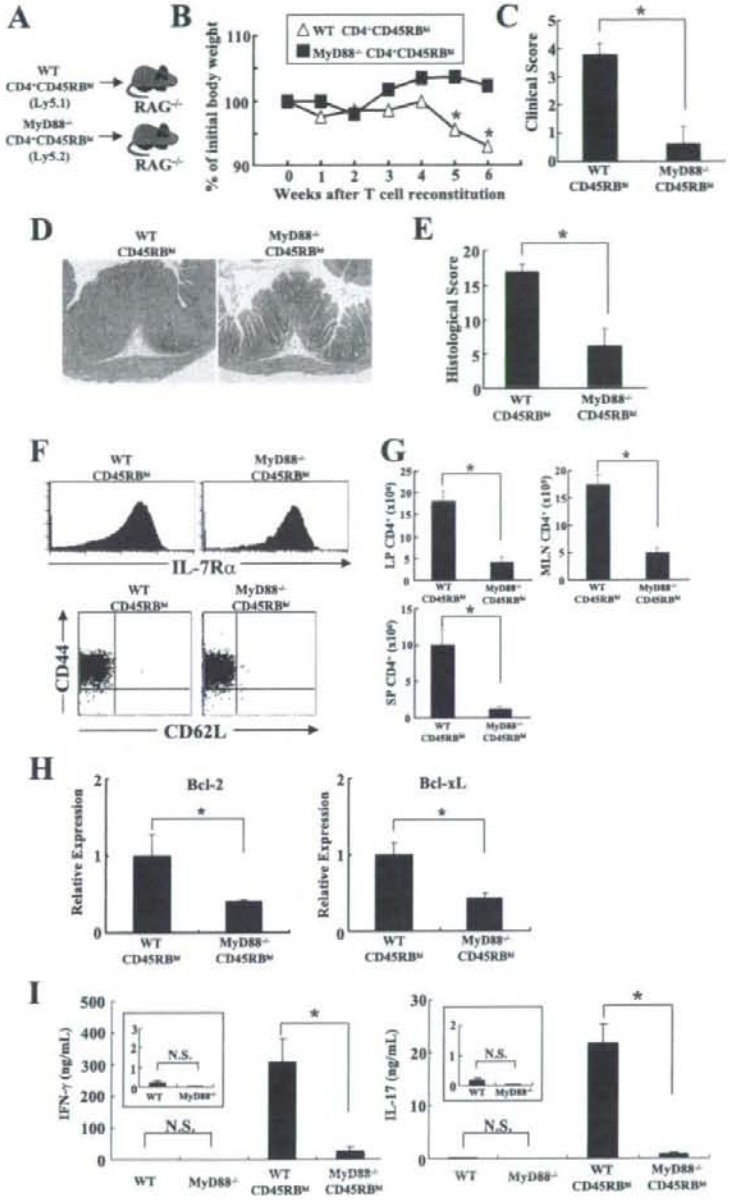

FIGURE 2. RAG-2$^{-/-}$ mice transferred with MyD88$^{-/-}$CD4$^+$CD45RB^{high} T cells develop milder colitis. *A*, RAG-2$^{-/-}$ mice were transferred with splenic MyD88$^{+/+}$ (WT) ($n = 6$) or MyD88$^{-/-}$ ($n = 6$) CD4$^+$CD45RB^{high} T cells (3×10^5 cells/mouse). *B*, Change in body weight over time is expressed as percent of the original weight. Data are represented as the mean ± SEM of six mice in each group. *, $p < 0.05$. *C*, Clinical scores were determined at 6 wk after transfer as described in *Materials and Methods*. Data are indicated as mean ± SEM of six mice in each group. *, $p < 0.01$. *D*, Histological examination of the colon from WT (*left*) or MyD88$^{-/-}$ (*right*) CD4$^+$CD45RB^{high} T cells at 6 wk after transfer. Original magnification, ×100. *E*, Histological scoring of mice transferred with WT or MyD88$^{-/-}$CD4$^+$CD45RB^{high} T cells at 6 wk after transfer. Data are indicated as mean ± SEM of six mice in each group. *, $p < 0.01$. *F*, Phenotypic characterization of LP CD4$^+$ T cells isolated from mice transferred with WT or MyD88$^{-/-}$CD4$^+$CD45RB^{high} T cells at 6 wk after transfer. *G*, LP, MLN, and SP CD4$^+$ T cells were isolated from mice transferred with WT or MyD88$^{-/-}$CD4$^+$CD45RB^{high} T cells at 6 wk after transfer, and the number of CD4$^+$ cells was determined by flow cytometry. Data are indicated as mean ± SEM of six mice in each group. *, $p < 0.01$. *H*, Expression of Bcl-2 and Bcl-x_L mRNAs in SP cells was determined by quantitative RT-PCR, and are shown as relative amount of indicated mRNA normalized by expression of β-actin. Data are represented as the mean ± SEM of six samples. *, $p < 0.05$. *I*, Cytokine production by LP CD4$^+$ T cells. LP CD4$^+$ T cells were isolated at 6 wk after transfer and stimulated with anti-CD3 and anti-CD28 mAbs for 48 h. IFN-γ and IL-17 concentrations in culture supernatants were measured by ELISA. Data are indicated as mean ± SEM of six mice in each group. *, $p < 0.01$. WT: healthy WT mice, MyD88$^{-/-}$: healthy MyD88$^{-/-}$ mice, WT CD45RB^{high}: RAG-2$^{-/-}$ mice transferred with WT CD4$^+$CD45RB^{high} T cells, MyD88$^{-/-}$CD45RB^{high}: RAG-2$^{-/-}$ mice transferred with MyD88$^{-/-}$CD4$^+$ CD45RB^{high} T cells.

performed in vivo competition experiments. The same number (2.0×10^5 cells/mouse) of colitogenic LP memory CD4$^+$ T cells obtained from colitic mice that were transferred with either MyD88$^{+/+}$ (Ly5.1$^+$) or MyD88$^{-/-}$ (Ly5.2$^+$) CD4$^+$CD45RB^{high} T cells from either MyD88$^{+/+}$ mice (Ly5.1$^+$) or MyD88$^{-/-}$ mice (Ly5.2$^+$) after 10 wk from transfer were coinjected i.p. into new RAG-2$^{-/-}$ mice ($n = 6$), and the mice were monitored for 6 wk after the retransfer.

In experiments 1–4, all mice were assessed for a clinical score (18) that is the sum of four parameters listed as follows: hunching and wasting, 0 or 1; colon thickening, 0–3 (0, no colon thickening; 1, mild thickening; 2, moderate thickening; 3, extensive thickening); and stool consistency, 0–3 (0, normal beaded stool; 1, soft stool; 2, diarrhea; 3, bloody stool) (18). To monitor the clinical sign during the observed period over time, the ongoing disease activity index is defined as the sum (0–5 points) of the above-mentioned parameters except the colon thickening.

Experiment 5. To assess the requirement of MyD88-dependent signaling for the lymphopenia-driven rapid proliferation (19) of colitogenic memory CD4$^+$ T cells, we performed a short-term observation of in vivo competition experiments in combination with the CFSE-labeling method. The same number (2.0×10^6 cells/mouse) of CFSE-labeled LP memory CD4$^+$ T cells from colitic mice that were initially transferred with MyD88$^{+/+}$ (Ly5.1$^+$) or MyD88$^{-/-}$ (Ly5.2$^+$) CD4$^+$CD45RB^{high} T cells at 10 wk after transfer were injected i.p. into new RAG-2$^{-/-}$ mice ($n = 6$). In experiment 5, mice were sacrificed 10 days after retransfer, and assessed for cell divisions by CFSE dilution.

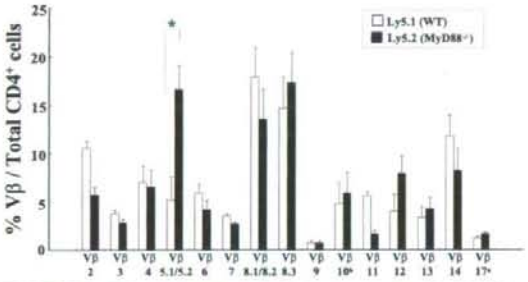

FIGURE 3. Vβ repertoire shows little difference between MyD88$^{+/+}$ or MyD88$^{-/-}$ donor cells. To analyze the TCR Vβ family repertoire, SP cells were isolated from mice transferred with Ly5.1^{+}MyD88$^{+/+}$ (WT) or Ly5.2^{+}MyD88$^{-/-}$CD4^{+}CD45RB^{high} T cells at 6 wk after transfer, and then triple-stained with PerCP-conjugated ant-CD3ε mAb (145-2C11), PE-conjugated anti-CD4 mAb (RM4-5), and a panel of 15 FITC-conjugated Vβ mAbs. Each percentage value indicates the frequency of each Vβ pooled from three independent experiments ($n = 6$). *, $p < 0.05$.

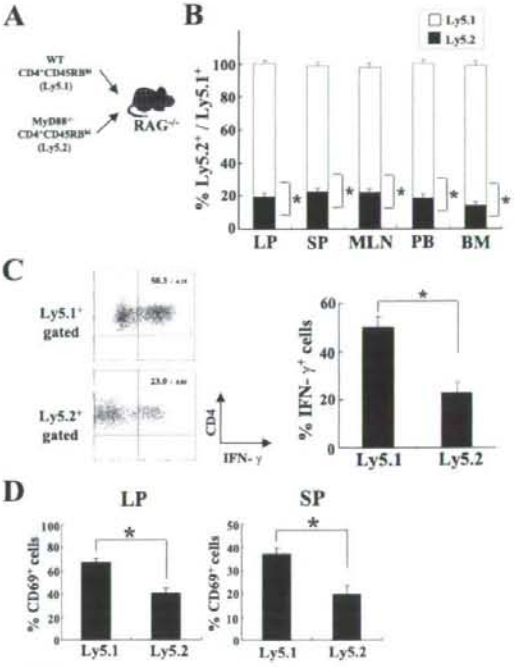

FIGURE 4. Expansive activity of MyD88$^{+/+}$ donor cells predominates over that of MyD88$^{-/-}$ donor cells in an in vivo competition assay. *A*, The same number (2.5×10^5 cells/mouse) of CD4^{+}CD45RB^{high} T cells from Ly5.1^{+}MyD88$^{+/+}$ (WT) mice and Ly5.2^{+}MyD88$^{-/-}$ mice was coinjected i.p. into RAG-2$^{-/-}$ mice ($n = 6$). *B*, Six weeks after transfer, LP, SP, MLN, PB, and BM CD4^{+} T cells were isolated, and the ratio of Ly5.1^{+} and Ly5.2^{+} CD4^{+} cells was determined by flow cytometry. *, $p < 0.01$. *C*, The frequencies of IFN-γ-producing LP CD4^{+} T cells per total Ly5.1^{+} or Ly5.2^{+} cells were analyzed in the indicated subpopulations by flow cytometry. Data are represented as mean ± SEM of three independent experiments. *, $p < 0.01$. *D*, Phenotypic characterization of LP and SP CD4^{+} T cells after transfer of CD4^{+}CD45RB^{high} T cells. % CD69^{+}, Percentages of CD4^{+}CD69^{+} cells per total CD4^{+} cells. Data are represented as mean ± SEM of six mice per group. *, $p < 0.05$.

Histological examination

Tissue samples were fixed by 10% neutral-buffered formalin, and paraffin-embedded sections (5 μm) were stained with H&E. Three tissue samples from the proximal, middle, and distal parts of the colon were prepared and subjected for analysis. The sections were analyzed without prior knowledge of the type of T cell reconstitution. The most affected area was graded by the severity of lesions. The degree of colonic inflammation was calculated using a previous scoring system (20): mucosa damage, 0; normal, 1; 3–10 intraepithelial cells (IEL)/high power field (HPF) and focal damage, 2; >10 IEL/HPF and rare crypt abscesses, 3; >10 IEL/HPF, multiple crypt abscesses and erosion/ulceration, submucosa damage, 0; normal or widely scattered leukocytes, 1; focal aggregates of leukocytes, 2; diffuse leukocyte infiltration with expansion of submucosa, 3; diffuse leukocyte infiltration, muscularis damage, 0; normal or widely scattered leukocytes, 1; widely scattered leukocyte aggregates between muscle layers, 2; leukocyte infiltration with focal effacement of the muscularis, 3; extensive leukocyte infiltration with transmural effacement of the muscularis.

Cytokine ELISA

To measure cytokine production, 1×10^5 LP CD4^{+} T cells were cultured in 200 μl of culture medium at 37°C in a humidified atmosphere containing 5% CO_2, using 96-well plates (Costar) which were precoated with 5 μg/ml hamster anti-mouse CD3ε mAb (145-2C11; BD Pharmingen) and hamster 2 μg/ml anti-mouse CD28 mAb (37.51; BD Pharmingen) in PBS overnight at 4°C. Culture supernatants were removed after 48 h and assayed for cytokine production. Cytokine concentrations were determined by specific ELISA following the manufacturer's recommendation (R&D Systems).

Flow cytometry

To detect the surface expression of molecules, isolated splenocytes, MLN, PB, BM, or LP mononuclear cells were preincubated with an FcγR-blocking mAb (CD16/32; 2.4G2; BD Pharmingen) for 15 min followed by incubation with specific FITC-, PE-, PerCP-, allophycocyanin- or biotin-labeled Abs for 20 min on ice. The following mAbs except biotin-conjugated anti-mouse IL-7Rα (A7R34; eBioscience) were obtained from BD Pharmingen; anti-CD3ε mAb (145-2C11), anti-CD4 mAb (RM4-5), anti-CD45RB mAb (16A), anti-CD62L (MEL-14), anti-CD44 mAb (IM7), anti-CD69 mAb (H1.2F3). Biotinylated Abs were detected with PE-streptavidin. Standard three- or four-color flow cytometric analysis was performed by the FACSCalibur equipped with CellQuest software. Background fluorescence was assessed by the staining of control irrelevant isotype. To analyze the TCR Vβ family repertoire, splenic cells were triple-stained with PerCP-conjugated anti-CD3ε mAb (145C-11), PE-conjugated anti-CD4 mAb (RM4-5), and either of the following FITC-conjugated mAbs: Vβ2; KJ25, Vβ3; KT4, Vβ4; MR9-4, Vβ5.1/5.2; RR4-7, Vβ6; TR310, Vβ7; MR5-2, Vβ8.1/2; B21.14, Vβ8.3; MR10-2, Vβ9; B21.5, Vβ10^{b}; RR3-15, Vβ11; MR11-1, Vβ12; IN12.3, Vβ13; 14.2, Vβ14; and KJ23, Vβ17^{a}. All the Abs were purchased from BD Pharmingen.

CFSE labeling of T cells

T cell division in vivo was assessed by flow cytometry of CFSE-labeled cells. Isolated LP CD4^{+} T cells were stained in vitro with the cytoplasmic dye CFSE (Molecular Probes) before reconstitution by incubation for 10 min at 37°C with 5 μM CFSE. The labeling reaction was quenched by washing in ice-cold RPMI 1640 supplemented with 10% FCS.

Statistical analysis

The results are expressed as mean ± SEM. Groups of data were compared by Mann-Whitney *U* test. Differences in data were considered to be statistically significant when $p < 0.05$.

Results

TLRs are expressed in CD4^{+}CD45RB^{high} donor cells and colitic LP CD4^{+} cells

To assess the direct involvement of TLR signaling in regulating cell function of CD4^{+} T cells composing chronic colitis under the presence of commensal bacteria, we examined whether mRNAs of TLR1–9 and their adaptor molecule, MyD88, are expressed in donor T cells or the LP CD4^{+} T cells in colitic RAG-2$^{-/-}$ mice transferred with CD4^{+}CD45RB^{high} T cells. To do so, we isolated

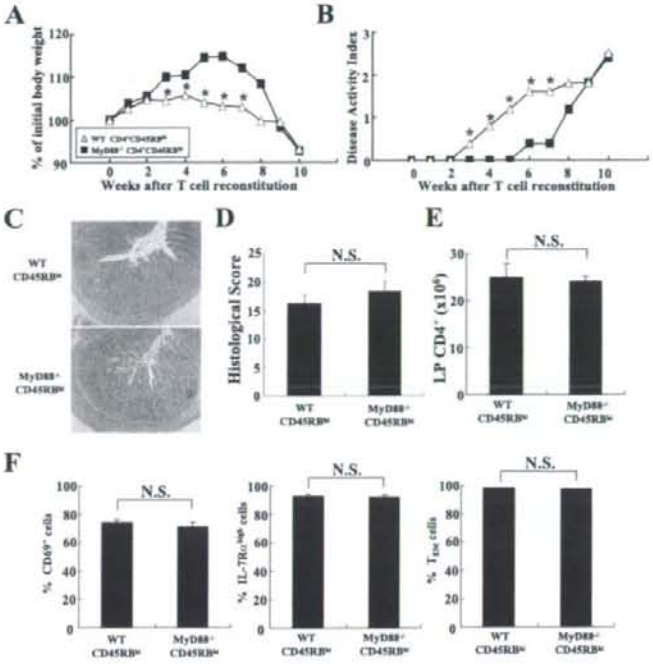

FIGURE 5. RAG-2$^{-/-}$ mice transferred with MyD88$^{-/-}$CD4$^+$CD45RB^{high} T cells develop colitis with the delayed kinetics, but reach to a similar level of mice transferred with MyD88$^{+/+}$CD4$^+$CD45RB^{high} T cells at 10 wk after transfer. *A*, Change in body weight is expressed as the percent of the original weight. Data are represented as mean ± SEM of five mice in each group. *, $p < 0.05$. WT, MyD88$^{+/+}$. *B*, Ongoing disease activity index was monitored during the course. Data are indicated as mean ± SEM of five mice in each group. *, $p < 0.05$. *C*, Histological examination of the colon from WT (*upper*) or MyD88$^{-/-}$ (*lower*) CD4$^+$CD45RB^{high} T cells at 10 wk after transfer. Original magnification, ×100. *D*, Histological scoring of mice transferred with WT or MyD88$^{-/-}$CD4$^+$CD45RB^{high} T cells at 10 wk after transfer. Data are indicated as the mean ± SEM of five mice in each group. *E*, LP CD4$^+$ T cells were isolated from mice transferred with WT or MyD88$^{-/-}$CD4$^+$CD45RB^{high} T cells at 10 wk after transfer, and the number of CD4$^+$ cells was determined by flow cytometry. Data are indicated as mean ± SEM of five mice in each group. *F*, Phenotypic characterization of LP CD4$^+$ T cells isolated from mice transferred with WT or MyD88$^{-/-}$CD4$^+$CD45RB^{high} T cells at 10 wk after transfer. The percentage of positive cells per total CD4$^+$ T cells (CD69$^+$/CD4$^+$, IL-7Rα$^+$/CD4$^+$, CD4$^+$CD44^{high}CD62L$^-$/CD4$^+$) was determined using flow cytometry.

each CD4$^+$ population under highly stringent gate definitions using FACSAria to avoid contamination of cells, such as macrophages, DCs, and B cells. As shown by RT-PCR in Fig. 1, whole splenocytes including T cells, B cells, macrophages, and DCs were used as the positive control, and expressed all members of TLR1–9 and MyD88. Under this condition, CD4$^+$CD45RB^{high} donor cells expressed MyD88 and TLRs except TLR-4, 5, and 9 along with MyD88, while colitic LP CD4$^+$ T cells expressed all members of TLRs and MyD88, indicating that TLR signaling via MyD88 may be directly involved in the priming, activation, proliferation, and survival of CD4$^+$ T cells in the present transfer model. The data were further by completely no detection of PCR products from a template prepared without the addition of reverse transcriptase, excluding a possibility of signals derived from contaminating genomic DNA rather than mRNA (data not shown).

RAG-2$^{-/-}$ mice transferred with MyD88$^{-/-}$CD4$^+$CD45RB^{high} T cells developed milder colitis

To explore whether the MyD88-signaling pathway in T cells is involved in the development of chronic colitis, we transferred MyD88$^{-/-}$ or MyD88$^{+/+}$ CD4$^+$CD45RB^{high} T cells into RAG-2$^{-/-}$ (MyD88$^{+/+}$) recipient mice maintaining an intact MyD88-dependent pathway of the innate immune system, meaning that only the transferred CD4$^+$ T cells lack the MyD88-dependent pathway within the recipient mice (Fig. 2*A*). When WT MyD88$^{+/+}$ CD4$^+$CD45RB^{high} cells were transferred into RAG-2$^{-/-}$ mice, the recipients rapidly developed severe wasting disease associated with clinical signs of severe colitis. Particularly, weight loss (Fig. 2*B*), persistent diarrhea and also occasionally bloody stool or anal prolapse was observed by tracking the clinical score up to 6 wk after transfer (Fig. 2*C*). However, when MyD88$^{-/-}$CD4$^+$ CD45RB^{high} T cells were transferred into RAG-2$^{-/-}$ mice, the recipients also developed wasting disease and colitis despite the delayed onset (see the following result in Fig. 5), but the clinical score at 6 wk after transfer was significantly lower as compared with that of mice transferred with control MyD88$^{+/+}$ CD4$^+$CD45RB^{high} T cells (Fig. 2*C*). Thus, the delayed onset and milder clinical score of mice transferred with MyD88$^{-/-}$CD4$^+$ CD45RB^{high} cells would easily be explained by the lack of a MyD88-dependent pathway in donor CD4$^+$ T cells, but not in other innate immune cells of the recipient mice.

At 6 wk after transfer, the colon from of mice transferred with MyD88$^{+/+}$ donor cells, but not that from mice transferred with MyD88$^{-/-}$ donor cells, was enlarged and had a greatly thickened wall (data not shown). In addition, the enlargement of the SP and MLN was also present in mice transferred with MyD88$^{+/+}$ donor cells as compared with mice transferred with MyD88$^{-/-}$ donor cells (data not shown). Histological examination revealed that mice transferred with MyD88$^{+/+}$ donor cells developed severe colitis showing prominent epithelial hyperplasia and erosion with a massive infiltration of mononuclear cells in LP of the colon (Fig. 2*D*). In contrast, mice transferred with MyD88$^{-/-}$ donor cells developed milder colitis as compared with mice transferred with MyD88$^{+/+}$ donor cells. This difference was statistically confirmed by histological scoring of multiple colon sections, which was mice transferred with MyD88$^{+/+}$ donor cells, 17.0 ± 1.0; and mice transferred with MyD88$^{-/-}$ donor cells, 6.2 ± 2.42 ($p < 0.01$) (Fig. 2*E*). Importantly, flow cytometry analysis revealed that the LP CD4$^+$ T cells isolated from recipients transferred with either MyD88$^{-/-}$ or MyD88$^{+/+}$ CD4$^+$CD45RB^{high} T cells were CD44^{high}CD62L$^-$IL-7Rα^{high} (Fig. 2*F*), indicating that the transferred CD4$^+$CD45RB^{high} T cells could differentiate into effector-memory T cells even in the absence of the MyD88-dependent pathway within colitic CD4$^+$ T cells.

A further quantitative evaluation of CD4$^+$ T cell infiltration was made by isolating LP, MLN, and SP CD3$^+$CD4$^+$ T cells. As shown in Fig. 2*G*, significantly lower numbers of CD4$^+$ T cells were recovered from LP, MLN, and SP of mice transferred with

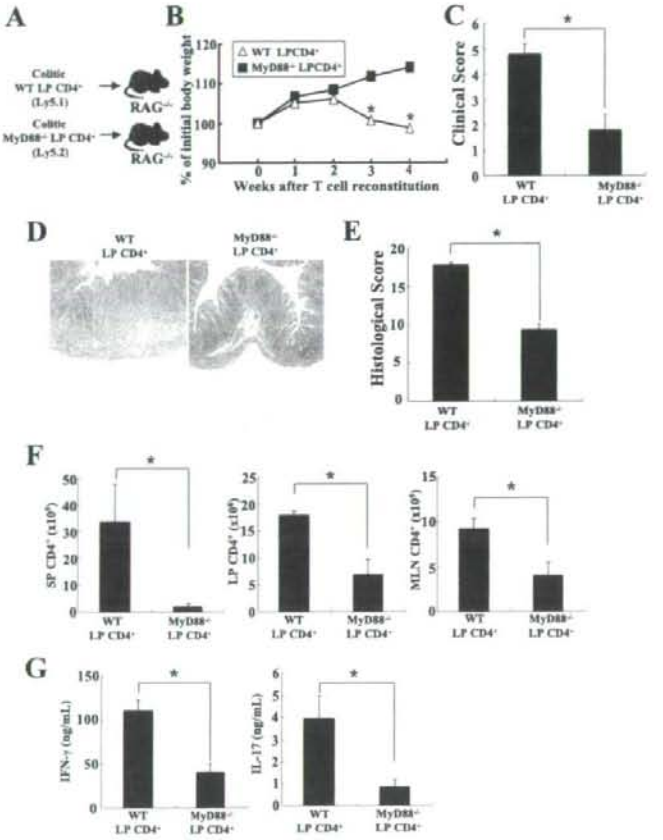

FIGURE 6. RAG-$2^{-/-}$ mice transferred with colitogenic MyD88$^{-/-}$ LP CD4$^+$ T cells develop milder colitis. *A*, RAG-$2^{-/-}$ mice were transferred with colitogenic MyD88$^{+/+}$ (WT) ($n = 6$) or MyD88$^{-/-}$ ($n = 6$) LP CD4$^+$ T cells (4×10^5 cells/mouse). *B*, Change in body weight is expressed as percent of the original weight. Data are represented as mean ± SEM of six mice in each group. *, $p < 0.05$. *C*, Clinical scores were determined at 4 wk after transfer as described in *Materials and Methods*. Data are indicated as mean ± SEM of six mice in each group. *, $p < 0.01$. *D*, Histological examination of the colon from mice transferred with colitic WT (*left*) or MyD88$^{-/-}$ (*right*) CD4$^+$ T cells at 4 wk after transfer. Original magnification, ×100. *E*, Histological scoring of mice transferred with colitic WT or MyD88$^{-/-}$CD4$^+$ T cells at 4 wk after transfer. Data are indicated as mean ± SEM of six mice in each group. *, $p < 0.05$. *F*, LP, MLN, and SP CD4$^+$ T cells were isolated from of mice transferred with colitic WT or MyD88$^{-/-}$CD4$^+$ T cells at 4 wk after transfer, and the number of CD4$^+$ cells was determined by flow cytometry. Data are indicated as mean ± SEM of six mice in each group. *, $p < 0.05$. *G*, Cytokine production by LP CD4$^+$ T cells. LP CD4$^+$ T cells were isolated at 4 wk after transfer and stimulated with anti-CD3 and -CD28 mAbs for 48 h. IFN-γ and IL-17 concentrations in culture supernatants were measured by ELISA. Data are indicated as mean ± SEM of six mice in each group. *, $p < 0.05$.

MyD88$^{-/-}$ donor cells as compared with mice transferred with MyD88$^{+/+}$ donor cells. To further address the survival of CD4$^+$ T cells, we next assessed whether regulation of Bcl-2 and Bcl-x_L expression requires the MyD88-dependent signaling pathway using a quantitative RT-PCR. As expected, the SP CD4$^+$ T cells from mice transferred with MyD88$^{-/-}$ donor cells expressed a significantly lower level of Bcl-2 and Bcl-x_L compared with those from mice transferred with MyD88$^{+/+}$ donor cells (Fig. 2*H*). We also examined the cytokine production by isolated LP CD4$^+$ T cells from recipient mice transferred with MyD88$^{+/+}$ or MyD88$^{-/-}$ donor cells along with LP CD4$^+$ T cells from healthy MyD88$^{+/+}$ or MyD88$^{-/-}$ mice. As shown in Fig. 2*I*, LP CD4$^+$ T cells from mice transferred with MyD88$^{-/-}$ donor cells produced significantly less IFN-γ and IL-17 as compared with those from mice transferred with MyD88$^{+/+}$ donor cells upon in vitro stimulation by anti-CD3/anti-CD28 mAbs. LP CD4$^+$ T cells from both healthy WT and MyD88$^{-/-}$ mice produced only a small amount of these cytokines, showing no significant difference under the same condition (Fig. 2*I*).

Vβ repertoire is almost constant regardless of WT or MyD88$^{-/-}$ donor cells

Although we found that mice transferred with MyD88$^{-/-}$ donor cells develop milder colitis compared with mice transferred with MyD88$^{+/+}$ donor cells, possibly due to the lack of a MyD88 pathway within CD4$^+$ T cells, it remained unclear whether expanded CD4$^+$ T cells in the recipient mice recognize the same antigenic epitopes of CD4$^+$ T cells. To clarify this issue, SP CD4$^+$ T cells from both groups of mice were analyzed for their TCR Vβ repertoire by flow cytometry. As shown in Fig. 3, the polyclonal dominant TCR Vβ repertoire with the dominancy of Vβ8.1/8.2 and Vβ8.3 was almost constant regardless of MyD88$^{+/+}$ or MyD88$^{-/-}$ donor cells. Only the frequency of Vβ5.1/5.2 in mice transferred with MyD88$^{-/-}$ donor cells was significantly increased as compared with that in mice transferred with WT donor cells, indicating that colitogenic CD4$^+$ T cells recognizing the same or similar Ag epitopes could develop independently from the TLR-MyD88 signaling pathway in CD4$^+$ T cells.

Expansive activity of WT donor cells predominates over that of MyD88$^{-/-}$ donor cells in in vivo competition assay

To further assess the requirement of TLR-MyD88 signaling for the expansion of CD4$^+$ donor cells, we performed in vivo competition experiments. The same number (2.5×10^5 cells/mouse) of CD4$^+$CD45RB^{high} donor cells from Ly5.1-background (Ly5.1$^+$) MyD88$^{+/+}$ and Ly5.2-background (Ly5.2$^+$) MyD88$^{-/-}$ mice were coinjected i.p. into the identical RAG-$2^{-/-}$ mice (Fig. 4*A*). As expected, recipient mice developed severe colitis at 6 wk after cotransfer (data not shown), and a significantly lower proportion of Ly5.2$^+$ MyD88$^{-/-}$ CD4$^+$ T cells was observed not only in the inflamed LP, but also in SP,